# EFFECTS OF METAL CATION ON THE SKELETAL ISOMERIZATION OF *n*-BUTENE OVER ZSM-5 AND FERRIERITE

**A Thesis Submitted to**
**the Graduate School of Engineering and Sciences of**
**İzmir Institute of Technology**
**in Partial Fulfillment of the Requirements for the Degree of**

**MASTER OF SCIENCE**

**in Chemical Engineering**

**by**
**Öniz BİRSOY**

**February 2005**
**İZMİR**

We approve the thesis of **Öniz BİRSOY**

**Date of Signature**

..... **09.02.2005**

**Assist. Prof. Dr. Selahattin YILMAZ**
Supervisor
Department of Chemical Engineering

..... **09.02.2005**

**Assist. Prof. Dr. Oğuz BAYRAKTAR**
Co-Supervisor
Department of Chemistry

..... **09.02.2005**

**Prof. Dr. Levent ARTOK**
Co-Supervisor
Department of Chemistry

..... **09.02.2005**

**Prof. Dr. Gönül GÜNDÜZ**
Department of Chemical Engineering, Ege University

..... **09.02.2005**

**Assist. Prof. Dr. Fehime ÖZKAN**
Department of Chemical Engineering

..... **09.02.2005**

**Assist. Prof. Dr. Erol ŞEKER**
Department of Chemical Engineering

..... **09.02.2005**

**Prof. Dr. Devrim BALKÖSE**
Head of Department

……..……..

**Assoc. Prof. Dr. Semahat ÖZDEMİR**
Head of the Graduate School

# ACKNOWLEDGEMENTS

I would like to express my gratitude to my advisor, Asst. Prof. Selahattin Yılmaz, for his guidance. I am grateful to Prof. Dr. Levent Artok for his valuable suggestions. I would like to thank Prof. Dr. Devrim Balköse for her understanding. I also would like to give my special thanks to Asst. Prof. Oğuz Bayraktar for his valuable recommendations and encouragement through my hardest times.

I would like to thank all of the experts in the Chemical Engineering Department of İzmir Institute of Technology, laboratory technicians and especially to the experts Nesrin Tatlıdil, and Özlem Çağlar for their contributions to the characterization studies.

I would like to acknowledge deeply to my roommates, Hilal Güleç, Belgin Tunçel and also Aslı and Özge Can for their friendships, supports and encouragements.

My special thanks go to my family for their endless support and understanding.

# ABSTRACT

The effects of metal cation on the skeletal isomerization of 1-butene to isobutene was investigated. H-ZSM-5 was sythesized with the initial $SiO_2/Al_2O_3$ ratio of 30. MFI-50, MFI-90 and Ferrrierite zeolite catalysts were commercially supplied. The zeolites were ion exchanged with cobalt, nickel, zinc, cupper (magnesium and manganese only for synthesized ZSM-5) salts, impregnated with cobalt, in order to change their acidity. The H-ZSM-5 zeolite was additionally ion exchanged with cobalt using different metal loading amounts. Then, the catalysts were tested for their activity in a fixed bed tubular quartz reactor at 375°C at weight hourly space velocity (WHSV) of 22 $h^{-1}$.

Scanning Electron Microscopy images and X-Ray Powder Diffraction patterns of the zeolites showed that their crystallinity was not affected with ion exchange, even with the increase in the loading amount (2.68 w%). But with the impregnation method, the intensity of the characteristic peaks for zeolites were decreased. Impregnating the zeolite also resulted in a decrease in the surface area.

The acidity measurements of the catalysts were made by IR spectroscopy with pyridine adsorption method. The tests showed that acidities of the catalysts were changed with ion exchange and impregnation of metal ions.

The catalytic tests for H-ZSM-5 showed that different metal loadings with ion exchange lowered the yield for isobutene. H-ZSM-5 showed a conversion of 59 % and 33.2 % yield for isobutene. The lowest yield was obtained from magnesium and manganese with 12.2 % and 9.6 %, respectively. The H-ZSM-5 zeolite catalysts were also tested for Co ion exchanged with different amounts (2.68, 1.45, 0.63 and 0.23 w%). 1.45 w% loaded catalyst showed the best activity for the reaction with a conversion of 59.1 %, and yield for isobutene 24.5 %. Both increased and decreased loading decreased yield 17.8 %, 2.5 % and 0.48 %, respectively. H-MFI-50 and its modified forms showed high conversions compared to H-ZSM-5. But low yields and selectivities were obtained. H-MFI-50 showed the highest conversion with 82.7 % and yield of 21.5 %. Co-MFI-50 showed similar conversion as the parent zeolite with 82.7 %, and yield of 17.9 %. The lowest conversion is obtained by Cu-MFI-50 with 76.5 % and yield for isobutene was 21 %. H-MFI-90 and its modified samples showed alike conversions around 76.1 %, but Cu loading decreased conversion as low as 65.9 %. Like MFI-50, the yield of isobutene was also affected by the metal ion exchanging. H-MFI-90 showed 24.8 %

yield of isobutene. However, Co-MFI-90 had a yield of 27.6 %. The worst yield was obtained from cupper loaded catalyst with 20.4 %. As would be expected, changing the metal ion loaded to ferrierite also changed the activity of the catalyst. The highest conversion was obtained by H-FER with 57 % and a yield of 39 %. Co-FER and Ni-FER showed similar conversions 52 % and 53 %, respectively. Zn-FER and Cu-FER showed the lowest conversions with 47 % and 45 %, respectively. Yields for the metal loaded catalysts lowered to 27 %.

Impregnation with Co, severely decreased the activity of the catalysts both compared to H form and ion exchanged form of the catalysts. Impregnated H-ZSM-5, H-MFI-50, H-MFI-90 and ferrierite showed conversions of 48.1 %, 66.8 %, 60.7 % and 45.4 %, respectively. The yields for isobutene were 11 %, 13.8 %, 15.5 % and 13.7 %, respectively.

# ÖZ

Metal katyonlarının n-bütenin iskelet izomerizasyonuna etkisi incelenmiştir. H-ZSM-5, sentez jelindeki $SiO_2/Al_2O_3$ oranı 30 olacak şekilde sentezlenmiştir. MFI-50, MFI-90 ve Ferrit zeolit katalizörleri ticari olarak temin edilmiştir. Zeolitlerin asitliklerinin değiştirilmesi amacıyla, kobalt, nikel, çinko, bakır (magnezyum ve manganez sadece sentezlenen ZSM-5 ile) tuzlarıyla iyon değişimi yapılmış, kobaltla emdirme uygulanmıştır. H-ZSM-5 zeolitina farklı kobalt miktarları kullanılarak iyon değişimi uygulamıştır. Ardından, katalizörlerin aktiflikleri sabit yataklı bir reaktör düzeneğinde 375°C de test edilmiştir.

Zeolitlerin taramalı elektron mikroskobu görüntüleri ve X-Ray kırınım desenleri kristalliklerininin iyon değişimi ile değişmediğini göstermiştir. Ancak emdirme yönteminin zeolitlerin karakteristik piklerini azaldığı görülmüştür. Emdirme yönteminde zeolitlerin yüzey alanında da azalma gözlemlenmiştir.

Katalizörlerin asitlik testleri, IR spektroskopi ile piridin adsorpsiyon yöntemi kullanılarak yapılmıştır. Test sonuçlarında katalizlerin metal iyonlarının iyon değişimi ve emdirme ile yüklenmesi sonucunda asitliklerinin değiştiği gözlemlenmiştir.

H-ZSM-5 katalizörünün aktivite testleri, farklı metallerin iyon değişimi ile yüklenmesinin izobüten verimini düşürdüğünü göstermiştir. H-ZSM-5 % 59 dönüşüm, % 33.2 izobüten verimi göstermiştir. En düşük verim magnezyum ve manganez yüklenmiş katalizörlerde elde edilmiştir, sırasıyla % 12.2 % ve % 9.6 %. Farklı miktarlarda (ağırlıkça % 2.68, % 1.45, % 0.63 and % 0.23) kobalt iyon değişimi uygulanmış H-ZSM-5 zeolit katalizörleride test edilmiştir. Ağırlıkça % 1.45 kobalt yüklenmiş katalizör en iyi aktiviteyi göstemiştir, % 59.1 ve % 24.5 izobüten verimi elde edilmiştir. Yükleme miktarının arttırılmasıda azaltılmasıda verimi düşürmüştür, sırasıyla % 17.8, % 2.5 ve % 0.48. H-MFI-50 ve metal yüklenmiş şekilleri H-ZSM-5'e göre daha yüksek dönüşümler göstermiştir. Ancak düşük verim ve seçicilikler elde edilmiştir. H-MFI-50, sırasıyla % 82.7 ve % 21.5 ile en yüksek dönüşümü ve verimi göstermiştir. Co-MFI-50, % 82.7 dönüşüm ve % 17.9 verim ile benzer bir aktivite göstermiştir. En düşük dönüşüm ve izobüten verimi sırasıyla % 76.5 ve % 21 ile Cu-MFI-50 katalizörü ile elde edilmiştir. H-MFI-90 ve metal yüklenmiş şekilleri benzer dönüşümler göstermişlerdir (yaklaşık % 76.1). Bakır yüklü katalizör % 65.9 dönüşüm ile en düşük aktiviteyi göstermiştir. MFI-50 de olduğu gibi izobüten verimi metal

yüklenmesinden etkilenmiştir. H-MFI-90 % 24.8 izobüten verimi göstermiştir. Ancak, Co-MFI-90 katalizörü ile % 27.6 verim elde edilmiştir. En düşük isobüten verimin bakır yüklü katalizör ile elde edilmiştir, % 20.4. Beklendiği gibi, metal yüklenmesi ferrierite katalizörlerinde aktivitesini etkilemiştir. En yüksek dönüşüm % 57 ile H-FER ile elde edilmiştir, verimi ise % 39 dur. Co-FER ve Ni-FER, sırasıyla % 52 ve % 53, benzer dönüşümler göstermişlerdir. Zn-FER ve Cu-FER, sırasıyla % 47 ve %45, en düşük dönüşümleri göstermiştir. Metal yüklü katalizörlerin verimi % 27 civarındadır.

Kobalt ile emdirme, katalizörlerin aktivitesini diğer katalizörlere oranla çok düşürmüştür. Emdirme yapılmış H-ZSM-5, H-MFI-50, H-MFI-90 ve ferrierite sırasıyla % 48.1, % 66.8, % 60.7 ve % 45.4 dönüşüm göstermişlerdir. İzobüten verimi ise sırasıyla %e 11, % 13.8, % 15.5 ve % 13.7 olarak bulunmuştur

# TABLE OF CONTENTS

# LIST OF FIGURES

**Figure** **Page**

# LIST OF TABLES

**Table** **Page**

# CHAPTER 1

# INTRODUCTION

The isomerization process involves the transformation of one molecular structure into another (isomer) whose component atoms are the same but arranged in a different geometrical structure. Since isomers may differ greatly in physical and chemical properties, isomerization offers the possibility of converting less desirable compounds into isomers with desirable properties, in particular to convert n-paraffins into iso-paraffins, thereby increasing the octane of the hydrocarbon stream.

In the production of MTBE (methyl *tert*-butyl ether) which is an oxygenate for production of unleaded gasoline, isobutene is used as a main reactant along with methanol (Seddon, 1992). The present sources of butenes including isobutene are mainly from by-products of thermal and catalytic crackers (Seddon, 1992; O'Young et al., 1993). Other possible sources are production by isomerization of *n*-butenes taken from thermal or catalytic crackers and dehydrogenation of isobutane taken from field butanes or produced by isomerization of *n*-butane (Seddon, 1992; O'Young et al., 1993; Sikkenga et al., 1984). However, these current supplies of isobutene is not sufficient to meet the increasing demand of MTBE. Therefore, considerable interest has been devoted to finding a new isobutene source via skeletal isomerization of n-butene (Szabo, 1991). and in the development of new skeletal isomerization catalyst and processes to give optimum results of various industrial requirements (O'Young et al., 1993).

The isobutene yield on the best contemporary catalyst is only about 40 % as a result of thermodynamical limitation at high reaction temperature (Houzvicka et al., 1997). Zeolite materials, especially in their hydrogen forms are known to behave quite effectively in catalyzing olefins (Houzvicka et al., 1997; O'Young et al., 1993; Bellussi et al., 1992). The most suitable zeolites for skeletal isomerization of *n*-butenes are in the group of 10-membered ring molecular sieves include ZSM-22, SAPO-11, ferrierite, and ZSM-5. Their pore sizes are suitable to achieve high activity and selectivity (Szabo, 1991; Xu, 1995; Seo, 1996). But, the ZSM-5 catalysts having channels formed by 10-

membered rings are very stable, but not selective (Houzvicka et al., 1997b; O'Young et al., 1993). Strong acidity and its high density of active sites are responsible for side products formation for ZSM-5. Therefore, modifying the acid strength of ZSM-5 as a potential way to increase the selectivity (Houzvicka, et al, 1997).

In this study, ZSM-5 and ferrierite zeolites were loaded with diffent metal cations by ion exchange and impregnation. The effects of different metal cations on the skeletal isomerization of n-butene were investigated.

# CHAPTER 2

# SKELETAL ISOMERIZATION OF LINEAR BUTENES OVER ZEOLITE CATALYSTS

## 2.1. The Kinetics and Mechanism of n-Butene Isomerization

The reaction mechanism of butenes has been subject to a lot of discussion (Houzvicka et al, 1997; Guisnet et al, 1998; Houzvicka et al, 1998). Thermodynamically, the formation of isobutene from n-butene is favoured at low temperature. However, in practice these lower temperatures will result in side reactions and as consequence the selectivity to isobutene is poor. Major side reactions that occur are dimerization to several octenes, cracking of these octenes to propenes and pentenes, hydrogen transfer and coking. The extent of undesired reactions can be decreased by applying low partial pressures of n-butene in the feed or by using high reaction temperatures. However, at higher temperatures the yield of isobutene is thermodynamically limited. Therefore, taking into account both, kinetics and thermodynamics, intermediate temperatures and low n-butene pressures are favoured resulting in high isobutene selectivities as well as high n-butene conversions.

It has been shown (Houzvicka et al., 1997; Meriaudeau, 1996) that n-butene reacts over acid catalysts with a monomolecular mechanism that results in the formation of isobutene very selectively (Reaction A in Figure 2.1), and with a bimolecular mechanism resulting in isobutene and cracking products, mainly propylene and pentenes (Reactions B in Figure 2.1). It is reasonable to think that the most selective catalysts for skeletal isomerization of n-butene are those over which the bimolecular mechanism is suppressed or at least minimised. The suppression of cracking by-products can be obtained either by adjusting the pore size of the catalyst, such that the bimolecular (2 $C4^+$) intermediate cannot form due to space constraints, or possibly by adjusting the acidity of the catalyst, such that the rate of formation of the $C4^=$ dimer intermediate is considerably lowered.

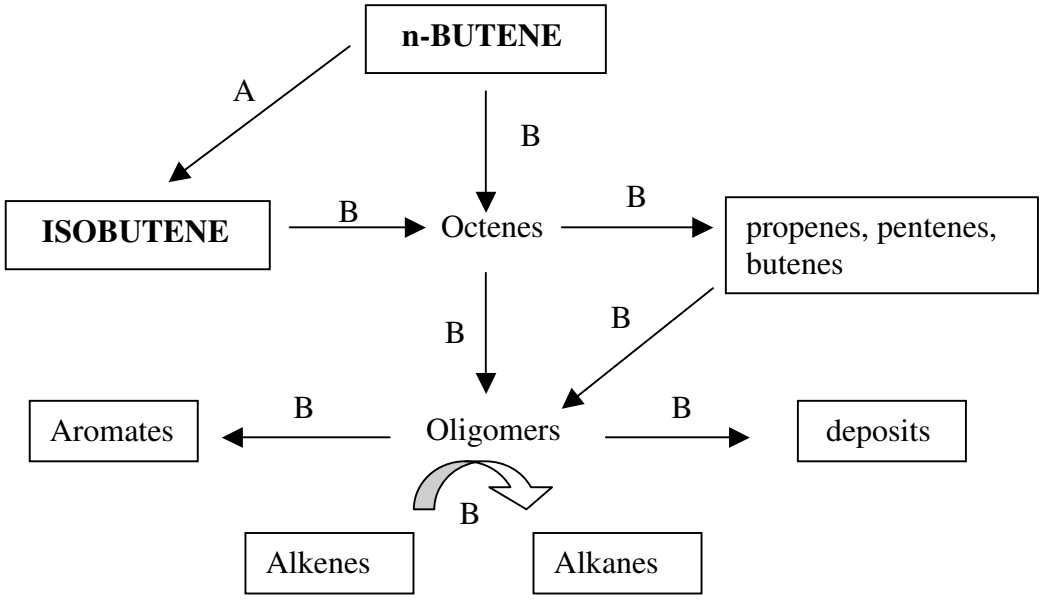


Figure 2.1. Scheme of n-butene reactions. A = the main desired reaction; B = the main undesired reactions (Houzvicka et al, 1997).

Three major types of reaction mechanism are proposed;

1) Bimolecular Mechanism;

Transformation of n-butene through the dimerization (1) - isomerization (2) - cracking (3) mechanism can be seen below (Guisnet et al, 1999).

Dimerization (1) and Cracking (3) steps: Steps A involve two tertiary carbenium ions as intermediates, steps B one tertiary and one secondary, steps C, two secondary carbenium ions. A is faster than B which is faster than C:

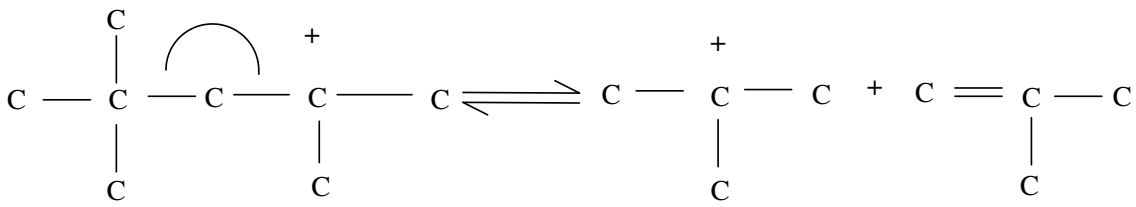

(A)

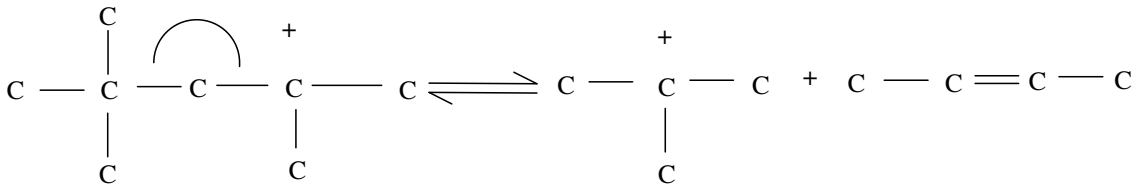

(B)

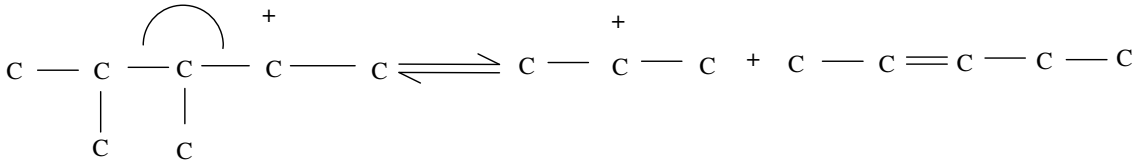

(C)

Isomerization steps (2): Alkyl shifts are responsible for isomerization without a change in the chain length:

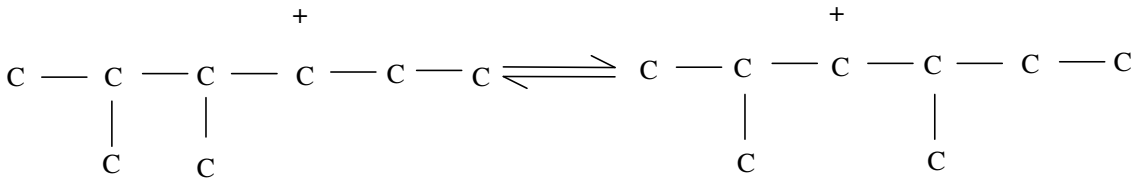

Changes in the chain length occur via protonated cyclopropane intermediates

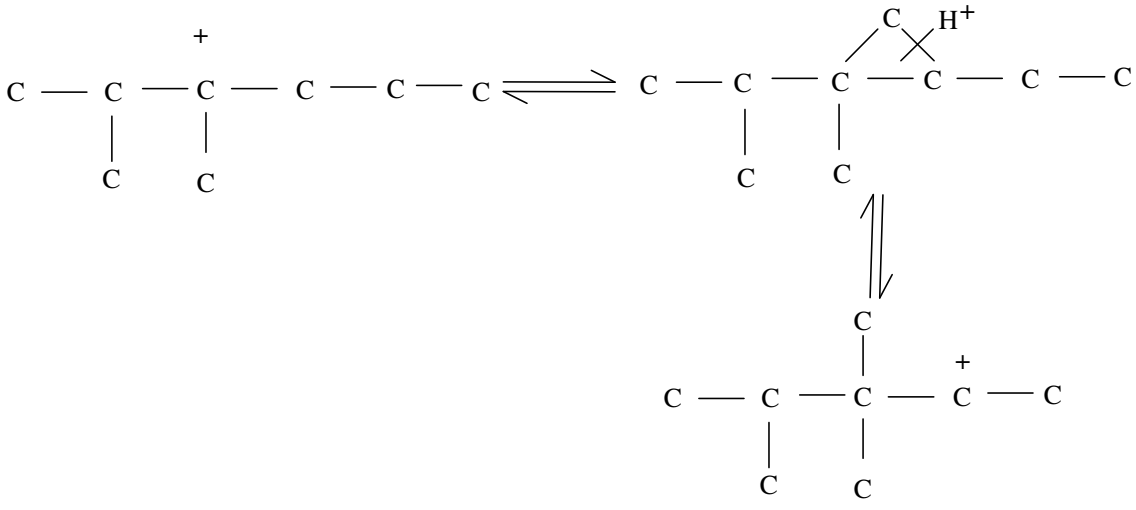

Through this mechanism, propene and pentenes are formed simultaneously with isobutene. Indeed dimethylhexenes and trimethylpentenes, which are the most likely

octene intermediates, undergo cracking not only into isobutene but also into propene plus pentenes. Moreover, the other possible $C_8$ intermediates, methylheptenes formed from dimerization of 1- butene, can only be cracked into propene and pentenes as shown above. Therefore the simultaneous formation of isobutene and propene and pentenes constitutes a strong argument in favour of the bimolecular mechanism in butene isomerization.

2) Monomolecular Mechanism;

In monomolecular mechanism, butene is isomerized over a plane Brønsted acid site, without the need of other butenes. The initial step of this reaction is the adsorption of butene on the Brønsted acid site resulting in a covalently bonded alkoxy-species. By proton-transfer from the zeolite to the hydrocarbon a cyclopropyl cation is formed, then followed by the energetically and thermodynamically highly unfavourable ring opening to the primary carbenium ion [101] leading to isobutene [102]. Monomolecular mechanism is summarized in Figure 2.2.

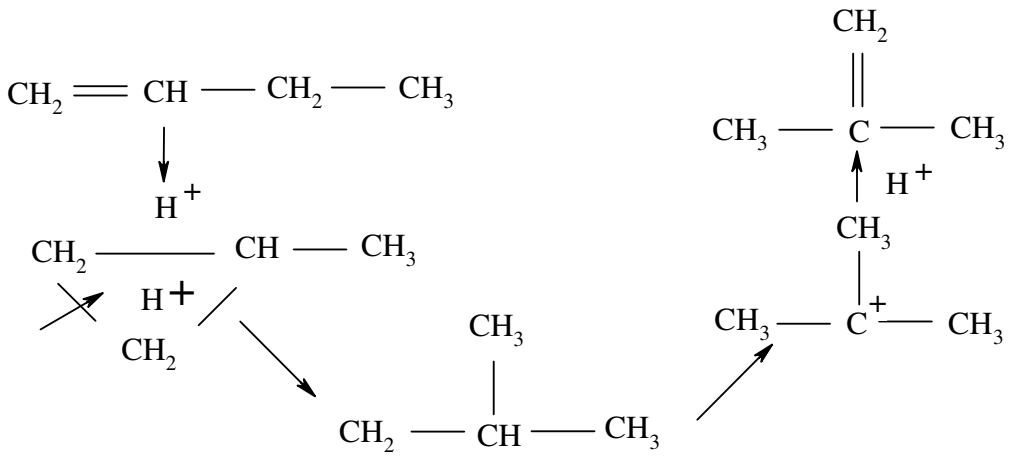

Figure 2.2. Monomolecular mechanism for the production of isobutene.

3) Pseudo-monomolecular Mechanism;

In pseudo-monomolecular mechanism involvement of a highly unfavourable primary carbenium ion is avoided. As depicted in Figure 2.3, the active site in this reaction pathway is formed by a carbenium ion that is fixed in the coke deposited on the catalyst with increasing time on stream. Butene reacts with this carbenium ion to give a secondary carbenium ion and after a methyl-and hydride shift a tertiary carbenium ion is

obtained. Finally intermediate produces an isobutene and with that the active site is regenerated.

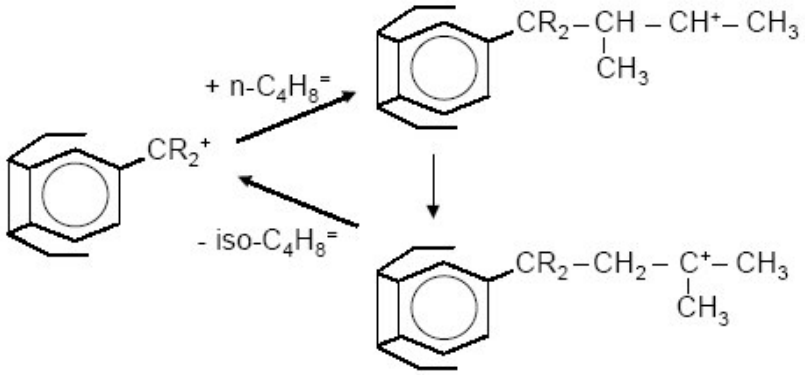


Figure 2.3. Pseudo-monomolecular reaction mechanism (Guisnet et al, 1997).

The acidity of the catalyst strongly influence the product selectivity. There are consecutive and parallel reactions occurring during n-butene isomerization that generally have a negative effect on isobutene selectivity. The most important competitive reactions are the dimerization of the olefins. Either n-butene, isobutene or both oligomerize forming $C_8$ products that are rapid to crack leading mainly to propylene and pentenes. It could be expected that the isomerization of n-butene and the oligomerization-cracking of the olefins require different acidities to proceed. Then, in principle, it should be possible, to change the product distribution by tailoring the acidity of the catalyst by controlling the number and strength of the acid sites.

The acid strength required for acid catalyzed conversions of hydrocarbons can be ranked as Cracking Oligomerization > Skeletal Isomerization >> Double Bond Isomerization. Therefore, an ideal skeletal isomerization catalyst should have an acidity that is strong enough for skeletal isomerization but not strong for oligomerization and cracking (Canizares et al, 2000 ).

It is investigated that the character of the acid sites, namely Brønsted and Lewis, are considered to affect the reaction pathway. Simultaneous presence of Brønsted and Lewis sites in zeolite lead to enhanced acidic activity of zeolites in hydrocarbon transformations. For 1-butene isomerization reaction, Lewis sites, if present with Brønsted sites in the zeolite, enhance dimerization and oligomerization of butenes. The formation of isobutene by skeletal isomerization of n-butenes was found to

be proportional to the concentration of Brønsted sites present in 10 member ring main channels of zeolites accessible to isobutene molecules (Wichterlova et al, 1999; Asensi et al, 1998).

Hydrocarbon conversions over microporous catalysts often lead to formation of some carbonaceous deposits, which may influence the catalytic action. The formation of carbonaceous deposits is a complicated process depending on several factors, like the nature of reactants and products, reaction temperature and time on stream. Moreover, for zeolites, the pore structure and the number, location and strength of the acid sites affect the coking behaviour of these materials.

## 2.2. Previous Studies on n-butene Isomerization

The skeletal isomerization of butenes has received much interest, not only from an industrial point of view but also scientifically, since it is a difficult reaction to catalyze. Several authors reported different catalysts for the reaction. However, the application of microporous materials as selective catalysts for butene skeletal isomerization opened a completely new field of research.

The most suitable materials for skeletal isomerization of *n*-butenes are the zeolite-type catalysts in the group of 10-membered ring (MR) molecular sieves include ferrierite, ZSM-22, SAPO-11, and ZSM-5. All of these catalysts are very stable, but the resulting yield and selectivity of the ZSM-5 are lower (Houzvicka et al., 1997). Strong acidity and its high density of active sites are responsible for side products formation (Houzvicka et al., 1997). The ZSM-5 catalysts having channels formed by 10-membered rings are very stable, but not selective (Houzvicka et al., 1997; O'Young et al., 1993).

Houzvicka et al.(1997,1998) demonstrated that the stability of the ZSM-5 catalyst is rather well, but selectivity to isobutene will always be low because of extensive oligomerization reactions. The shape selectivity of the ZSM-5 zeolite, consisting of a two-dimensional pore system with only 10 MR channels that are somewhat larger than the ferrierite 10 MR channels, is apparently not sufficient to form isobutene selectively. Acidity of ZSM-5 may not be appropriate as well, which therefore may cause the formation of by-products.

It has been shown that *n*-butene reacts over acid catalysts with a monomolecular mechanism that results in the formation of isobutene very selectively, and with a bimolecular mechanism resulting in isobutylene and cracking products, mainly propylene and pentenes. A good way to control the acidity of zeolite catalysts and therefore, their activity and selectivity is to modify the framework Si/Al ratio. It is well known that, in particular, the higher the Si/Al ratio of the zeolite framework, the lower the acid site density and the lower the coking rate will be and, and consequently, the lower the deactivation. (Canizares et al,2000).

Xu et al (1995) has shown that ferrierite is a shape selective catalyst for skeletal isomerization of n-butene to isobutene. As high as 36% yield and 90% selectivity to isobutene have been achieved. Also, their results suggested that side reactions for n-butene isomerization are mainly controlled by acidity and limitations of pore size.

Yang et al (1999) studied 1-butene isomerization over aluminophosphates molecular sieves and zeolites. They concluded that the acidic site of medium strength is responsible for the high selectivity (63.2 %) of SAPO-11. Metal ion exchanged into SAPO-11 or impregnated into SAPO-11 or $AlPO_4$-11 is less selective for isobutene.

Finelli et al (2003) studied ammonium, protonic and potassium ferrierites, which were impregnated with tungsten species. The catalytic behavior of samples with and without tungsten during the linear butene isomerization reaction was studied. The effect of both pretreatment and operational conditions over catalytic performance and deactivation of materials was also addressed. All the different results obtained explained with the weakened or strengthened acid sites.

Nieminen et al (2003) studied the role of copper in the skeletal isomerization of 1-butene over copper-modified mesoporous MCM-41 molecular sieve and Beta zeolite. The copper form of the catalysts were prepared by ion exchange using an aqueous solution of copper nitrate. Introduction of copper into MCM-41 enhanced the catalytic activity compared to the proton form of MCM-41. In disagreement to MCM-41, copper exchange in HBeta did not have any effect at all on the catalytic activity. This difference between the catalysts was explained by the strong acidity of H-Beta. Even, after ion exchange with copper nitrate, there were still several (strong) Brønsted acid sites left.

Lee et al (2002) studied skeletal isomerization of 1-butene to isobutene over various metal-cation-exchanged natural clinoptilolite zeolites. Cobalt-cation-exchanged natural clinoptilolite zeolite showed higher selectivity to isobutene in the skeletal

isomerization of 1-butene compared with that of proton-form natural clinoptilolite at the same conversion of *n*-butenes under the same reaction conditions. In the study, this high selectivity for cobalt-exchanged zeolite was explained by the selective elimination of strong acid sites that could give rise to the undesired side reactions.

## 2.3. Suggested Study

Zeolites have been widely used as catalysts for the isomerization of of n-butenes, since some undesirable side effects observed with other catalysts.

Their pore sizes are suitable for achieving high activity and selectivity. Also zeolites with suitable acidity are effective for this reaction. Medium pore 10 MR zeolites were predicted to be more selective than large pore 12 MR structures. They show good performance allowing yields of isobutene close to the thermodynamic limits under severe operating conditions. Furthermore, there appear to be large differences in product selectivity between 10 MR zeolites depending on the particular topology of the zeolite structure. For instance, unidirectional 10 MR zeolites, such as theta-1, ZSM-22 and ZSM-23 are more selective than ZSM-5, the latter having a bidirectional system of intersecting 10 MR channels. Other types of medium pore zeolites such as TON, AEL were also reported to be good catalysts. In contrast to TON and AEL, FER contains a two-dimensional pore system, where 8 and 10 member ring MR channels are perpendicularly interconnected. Although it is realized that pore dimensions are crucial, it is unclear to present, whether or not the additional eight MR channels (side channels) in FER contribute to the selective isomerization reaction. (Pál-Borbély et al, 1998; Domokos et al, 2000; Ahedi et al, 2001).

However, 10-membered ring channels have an oval shape and are too narrow for isobutene. Due to large cavities formed in the place of intersections of these cannels ZSM-5 shows low selectivity toward isobutene. Cavities offer enough space for extended dimerization and the by-products formation. Otherwise, ZSM-5 is very resistant against coking. On the other hand, ZSM-5 is an attractive catalyst for skeletal isomerization of n-butene because of its high stability and its availability, if only, its selectivity could be increased (Houzvicka et al, 1997).

The information given in literature showed that zeolite acidity and pore size are important for an active and selective catalyst. As mentioned before, 10 MR zeolites

were shown to be good catalysts for skeletal isomerization reaction. The possibility of improving the catalytic properties of zeolite in the isomerization of n-butene and effect of acidity on this reaction was investigated.

From the literature findings it was decided to study with ZSM-5 and ferrierite as zeolite supports.

## 2.3.1. Properties of Zeolites Used in this Work

### 2.3.1.1. ZSM-5

ZSM-5 is an abbreviation for Zeolite Socony-Mobil-5 which is a silica-rich synthetic prorotecto silicate of the Pentasil type (Figure 2.4). ZSM-5 is a bidirectional zeolite; its structure is formed by two systems of oval channels, one straight (5.2 × 5.7 Å), the other sinusoidal (5.3 × 5.6 Å). Its crystals are orthorhombic (Figure 2.5). The framework of ZSM-5 is made up of a unique configuration of silica and/or alumina tetrahedral consisting of eight 5-membered rings. They are zeolites with Si/Al ratio higher than 15, which makes these zeolites have hydrophobic characteristics. ZSM-5 is also is a coke resistant catalyst in the presence of olefins.

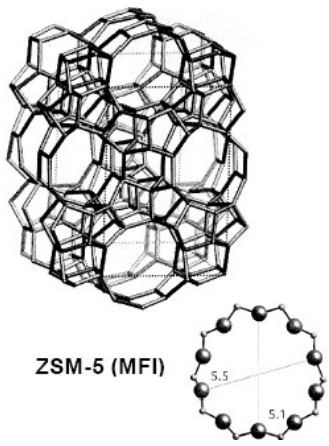


Figure 2.4. Framework structure of ZSM-5. (The ring structure of the main channel with its size is also visualized).

However, the selectivity to isobutene in butene skeletal isomerization for this zeolite is low, partly because the strong acidity and medium-size pore of ZSM-5 catalyzes side reactions, such as butene dimerization followed by cracking to light hydrocarbons.

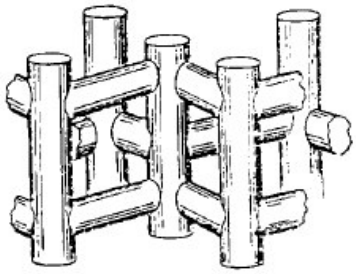

Figure 2.5. The channel structure in ZSM-5.

### 2.3.1.2. Ferrierite

The zeolite ferrierite (FER) is a molecular sieve with small pores and an orthorhombic framework. Its structure contains one-dimensional channels of 10-membered rings (4.2 × 5.4 Å) and one-dimensional channels of eight-member rings (3.5 × 4.8 Å) (Figure 2.6). These two kinds of channels are perpendicularly intersected. The eight-member ring channels contain spherical cavities with a size of about 6–7 Å.

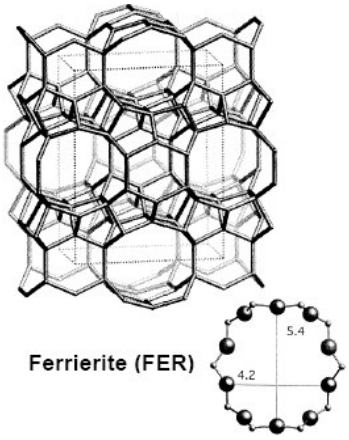


Figure 2.6. Framework structure of ferrierite. (The ring structure of the main channel with its size is also visualized).

Ferrierite (FER) was found to be even more selective than the 10 MR zeolites, affording high yields of isobutene with high selectivity. This peculiar catalytic behaviour has been related to its particular pore topology.

Ferrierite minerals has a Si/Al ratio in the range 4-7 and is considered one of the most siliceous naturally occurring zeolites. Because of their relatively high Si/Al ratio they have good acid and thermal stability. They can be synthesized using inorganic or organic bases. Ferrierite can also be prepared in its siliceous form by both aqueous and nonaqueous routes. Some synthesis methods, depending on the initial reactant composition give pure ZSM-5 or ferrierite or admixtures of ZSM-5 and ferrierite. Synthetic zeolites with the ferrierite type of framework (FER) include patented zeolite species like ZSM-21, ZSM-35, ZSM-38, FU-9.

The structural features make the zeolite ferrierite adequate to be use as a shape-selective catalyst in application to skeletal isomerization of *n*-butenes to isobutene, avoiding side-reactions such as dimerization or oligomerization of the feed and/or isobutene. Besides the pore size, the catalyst acidity is another factor affecting the selectivity to isobutene in butene skeletal isomerization. The ferrierite zeolite in the H-form presents strong acid sites (Brønsted), and the coke deposition observed during the *n*-butene isomerization on its pore structure leads to suppression of dimerization reactions by poisoning the strong acid sites and modifying the space around acid sites (Guisnet et al, 1998).

### 2.3.2. Modification of Zeolites

An essential step in the preparation of an active, stable zeolite catalyst is the modification of the material.

The porous structure of zeolites with large intracrystalline volumes and high surface areas per unit weight can be used to support catalytic active material. In this way a bifunctional catalyst can be obtained which combines the catalytic properties of the zeolite, including the sieve function, with the properties of the introduced catalytic material.

It is well-known that the catalytic behaviour of ZSM-5 can be modified by incorporation of metals in order to obtain catalysts for selective hydrocarbon

conversions (Hoang et al., 1994). The composition of the reaction products is linked to the reaction temperature and the relative strength of the hydrogenation and cracking activities in the catalysts, acid-metal balance, determined by the nature of the acid support and the hydrogenating function as well as the preparation method (Gil et al., 1994).

A good way to control the acidity of zeolite catalysts, their activity and selectivity is to modify the framework Si/Al ratio. It is well known that, in particular, the higher the Si/Al ratio of the zeolite framework, the lower the acid site density and the lower the coking rate will be and, and consequently, the lower the deactivation. The concentration and type of acid sites needed to improve isobutene selectivity. Dealumination is the removal of framework aluminum atoms without destroying the micropore structure. It is a way used to reduce the Bronsted strong acid sites in zeolites, removing framework Al and, consequently, increasing the framework Si/Al ratio. It is generally carried out through hydrothermal treatment (Baek et al, 1998). It can be achieved by hydrolysis of the Al – O - Si bonds by acid leaching combined with steaming, by complexation of the aluminum by oxalic acid and by direct replacement of aluminum by silicon with removal of framework aluminum atoms without gaseous silicon tetrachloride (Müller et al, 2000). However, with this method, there is a deposit in the pores and on the outer surface of crystallities of the aluminum species extracted from the zeolite framework, which can limit or block access to the acid sites.

Isomorphous substitution is the introduction of heteroatoms, such as B, Ga, Fe and Zn, etc., into the framework of the zeolite by the replacement of Si atoms. An interest arises to isomorphously substituted zeolites because the heteroatoms help in fine-tuning the strength of the acid sites and in introducing bifunctional features to zeolite catalysts.

The preparation method of bifunctional catalysts is as important as the chemical composition, setting both catalyst properties (Sivasanker and Ratnasamy, 1990). The objective of a preparation method is to distribute the active phase (metal) over the support in the most efficient way, highly dispersed, to obtain large specific surface areas and thus the maximum activity per weight of active compound over the support surface. The dispersion of the metal and its stability depend on the metal-support interaction. To manufacture catalysts in an efficient and reproducible process, it is essential to gain the control over parameters like the loading, dispersion, and location of the metal in the

catalysts. Several types of preparation techniques may be used (Foger, 1984; Stiles, 1987; Satterfield, 1991):

- mechanical mixing of metal compound and support,
- ion exchange processes,
- coprecipitation of metal oxides and support,
- impregnation processes, etc.

The metal distribution is mainly determined by the preparation method, but the nature of the metal precursor compound has also an important effect over the relationship between acid and metallic functions, determining the state of the metal (Gil et al., 1994; Rynkowski et al., 1993; Bartholomew et al., 1980; Campelo et al., 1982; Satterfield, 1991). The acid and metal site density and strength distribution are both important, and their proper balance is critical in determining the reactivity and selectivity of bifunctional catalysts.

### 2.3.2.1. Ion Exchange

Ion exchange describes a process by which ions are transferred from a solid phase to liquid phase and from liquid phase to solid phase simultaneously. It can be simply explained by "sponge model". In this model, ion exchanger is thought as a sponge with counter ions (exchangeable ions) floating in the pores. When the sponge is immersed in a solution, counter ions can leave the pores and float out. However, to preserve electroneutrality another counter ion from the solution enters the sponge and takes its place in compensating of the framework charge. As described in this picture, ion exchange concept can be given by the "redistribution of ions" (Helfferich 1962). The method of ion exchange allows for the introduction, in a controlled way, of a precursor from aqueous solution onto the support.

Ion-exchange is accomplished through contacting the zeolite with a salt solution which contains a large excess of the desired cations. Ion-exchange usually involves an aqueous solution containing the chloride, nitrate, or sulfate salt of the desired cation.

The ion exchange behaviour of the zeolite depends on upon (Breck, 1974):

1. The nature of the cation species, the cation size both anhydrous and hydrated, and the cation charge
2. The temperature

3. The concentration of the cation species in solution
4. The anion species associated with the cation in the solution
5. The solvent
6. The structural characteristics of the particular zeolite.

Catalyst systems, which require charge compensating ions as versatile materials suitable for ion exchange, include zeolites, cationic clays, and layered double hydroxides. Zeolites are cationic exchangers. Also, zeolites have unusual cation selectivity superior to the other exchangers. They combine the unique features of high ion exchange capacity, crystalline structure, and uniform pore sizes. Main difference in the ion exchange behaviour of zeolites and other exchangers (clay minerals and resins) is the microporous crystalline nature of zeolites. Since the microporous channels in the zeolite are comparable size to typical cation size, cations may be excluded from all or part of the internal surface of the zeolite on the basis of their size (Townsend, 1991). The catalytic properties of noble and transition metals and steric constraints imposed by the zeolite structure have provided a strong incentive for developing reliable procedures to prepare highly selective supported-metal catalysts with narrow particle size distributions (Schwarz, 1995). Because of their three-dimensional framework structure most zeolites do not undergo any structural changes with ion exchange (Breck, 1974).

In addition to producing changes in the chemical composition and resulting catalytic activity, ion exchange can also be used for these materials as a method to modify the size and accessibility of the internal pores, i.e., the secondary structure.

## 2.3.2.2. Impregantion

The mounting of dissolved aqueous precursors on oxide supports is generally accomplished by the so called impregnation method. This term denotes a procedure whereby a certain volume of solution containing the precursor of the active element of the catalyst is contacted with the solid support. The metal loading in the finished catalyst is typically 1-5 %.

When liquid is slowly added to a porous solid powder, the liquid is first absorbed in the pores and the powder will flow as if it is dry. When the pores have been filled the outside of the grains rather suddenly become wet, the grains will tend to stick

together and the powder will form lumps instead of flowing freely. The situation when the pores have been filled but the outside of the grains is dry is called incipient wetness and can easily be detected by shaking or stirring the powder. In this case the volume of solution either equals or is less than the pore volume of the support (Richardson, 1992).

When the interaction strength of the active precursor in solution with the support is weak, the method of incipient wetness impregnation followed by drying may be used to apply high loadings of precursors; the maximum loading is limited by the solubility of the precursor in the pore filling solution. On the other hand, increasing the weight loading requires higher concentrations results in lower solution pH and, in turn, may cause support disruption and substitution of ions into the support lattice. However, in the absence of sufficiently strong interactions, the drying step usually results in severe redistribution of the impregnated species, and the support can become heterogeneously covered by the active material in the final catalyst.

Catalysts are prepared by impregnation by spraying a solution of a metal salt onto powder porous support until incipient wetness. The catalysts are then dried and calcined to transform the metal into insoluble form.

The metal salt can be deposited homogeneously through the catalyst or most of the metal may be deposited near the outside of the catalyst.

Impregnation offers a number of advantages

- The filtering and the wash of the catalyst are eliminated.
- Small metal loadings are easily prepared.
- Impregnation offers some control over the distribution of the metal.

and disadvantages

- High metal loadings are not possible.
- A good impregnation solution may be impossible to find.

In the wet impregnation technique (also called soaking or dipping), an excess of solution is used. After a certain time, the solid is separated from solution, and the excess solvent is removed by drying. The amount of the active precursor mounted onto the porous carrier, its concentration profile within the carrier grains, and its chemical environment on the support surface depend significantly on the conditions during these first two steps in catalyst preparation. Under equilibrium conditions, the amount introduced onto the porous support depends on the equilibrium concentration of the impregnating solution, the porous volume of the carrier, and the adsorption isotherm which describes the binding of the precursor onto the support surface.

# CHAPTER 3

# ZEOLITES

## 3.1. Industrial Importance of Zeolite Catalysts

Zeolites may be either obtained from mineral deposits or synthesized. Over 150 species of synthetic zeolite have been synthesized and 7 kinds of mineral zeolites have been found in substantial quantity and purity.

The major factors that determine commercial use of zeolites are (Breck 1980);
(1) structural chemistry,
(2) availability, and
(3) cost.

Zeolites are used in very different fields where advantage is taken of the specific properties of zeolitic materials. They are primarily used as adsorbents, catalysts, and ion exchangers. Zeolites play an important role in the petroleum and refining industries because of their strong acidity and/or their size selectivity (Armor 1998). Natural zeolites are mainly used in building (cements) or in paper industry (fillers for paper). Other applications of these materials are as cat litter, sewage water treatment and in agriculture. The by far largest amount of synthetic zeolites is used as ion-exchanger (water softener) in builders for detergents. Within the last 30 years, zeolites replaced most phosphates and complexing agents from detergents. Detergent builders are high performance materials which contain about 15-25 % of zeolite (Zeolite A). In petrochemical processing, zeolites are used as catalysts for Fluid Catalytic Cracking (FCC process), a process which transforms long-chain alkanes (heavy oil) into shorter ones (petrol), and to enhance the octane number of the petrol by producing branched species. In terms of volume, most of the zeolite catalysts are used in oil refining where Zeolite Y is employed on a large scale in catalytic cracking (Maxwell and Stork 1991). Other applications are hydrocracking (Zeolite Y, Mordenite), hydro-isomerization and dewaxing (Mordenite and ZSM-5) (Moscou 1991).

Catalysis is not the largest market segment of zeolites but it is the most valuable one. Zeolites are very efficient and selective catalysts for various reactions, especially in the petrochemical industry. The selectivity of zeolites is due to the limited pore sizes which only allow specific molecules either to enter the pores (educt selectivity) or to leave the pores (product selectivity) depending on their size. Furthermore, not every transition state during a reaction might be possible, thus, forcing a reaction only into one direction (restricted transition-state selectivity).

Zeolites have the ability to act as catalysts for chemical reactions which take place within the internal cavities. An important class of reactions is that catalysed by hydrogen-exchanged zeolites, whose framework-bound protons give rise to very high acidity. This is exploited in many organic reactions, including crude oil cracking, isomerization and fuel synthesis. Zeolites can also serve as oxidation or reduction catalysts, often after metals have been introduced into the framework. Examples are the use of titanium ZSM-5 in the production of caprolactam, and copper zeolites in $NO_x$ decomposition.

The fastest growing market, high-tech synthetic zeolite catalysts, hold the industry's future in the conversion of methanol to high quality gasoline, free from sulfur and nitrogen, or in products that improve the octane rating of gasoline without the use of lead. Mobil produced the first zeolite-based, oil- cracking catalyst in 1962, revolutionizing the petroleum industry worldwide by increasing the yield of gasoline from crude petroleum. In the chemical industry, these catalysts have become indispensable in many processes, including those involved in making polyester and plastics.

The zeolite market showing the different market segments is shown in Figure 3.1. As can be seen, the catalytic application of zeolites is only a small segment, but zeolite catalyst have more than 55 % of the market on a cash base. The products obtained by using these catalysts have a value which is several magnitudes higher than that of the catalysts themselves, thus making them extremely important for many processes.

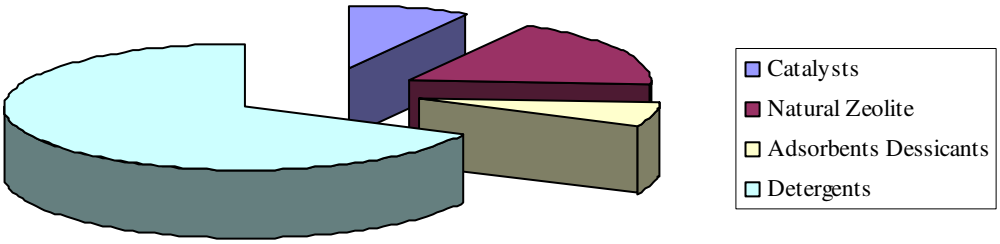


Figure 3.1. Catalytic applications of zeolites (Karge et al, 1999)

## 3.2. Zeolite Chemistry

Zeolites are members of a family of minerals called "tectosilicates," which includes dense-phase materials such as the feldspars and the various forms of silica. They are microporous, high-internal-surface-area crystalline materials. Their crystal structure is based on a three dimensional framework of $(SiAl)O_4$ tetrahedra with all four oxygens shared by adjacent tetrahedra (Figure 3.2).

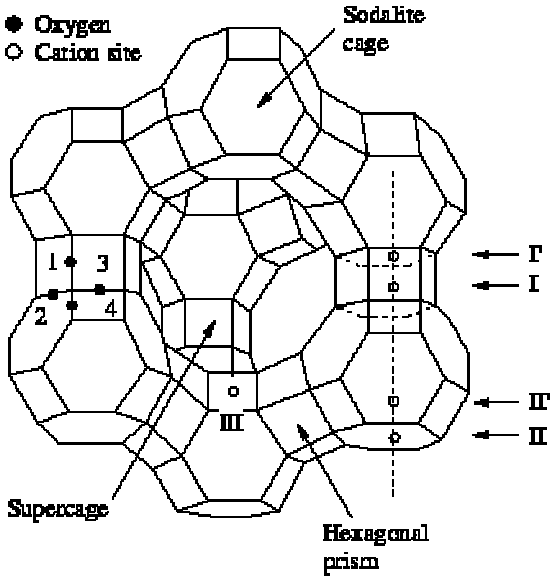


Figure 3.2. Diagram showing the differing oxygen and cation locations (framework structure of faujasite).

The tetrahedra make up three-dimensional network structures to form channels and cages or cavities of discrete size (Weitkamp, 1998).

The structural formula of a zeolite is best expressed for the crystallographic unit cell as:

$$M_{(x/n)}\,[(AlO_2)_x\,(SiO_2)_y\,] \cdot mH_2O$$

In this formula, M represents the cation of valence n and x is generally equal to or greater than 2 since $AlO_4$ tetrahedra can join only to $SiO_4$ tetrahedra. The structural formula of a zeolite may be best expressed by the idealized formula for the crystallographic unit cell where m is the number of water molecules and the ratio y/x varies between 1 and 5 depending on the structure. The sum (x + y) represents the total number of tetrahedra, while the portion with [ ] defines the framework composition (Breck 1974, Tsitsishvili et al. 1992).

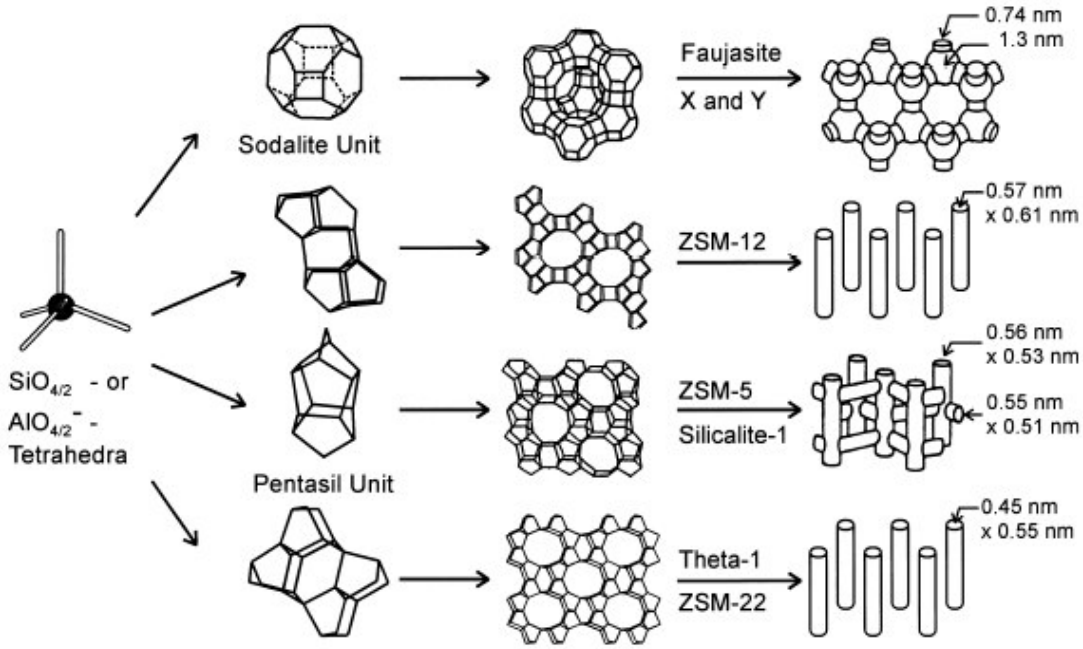


Figure 3.3. Structures of four selected zeolites (from top to bottom: faujasite or zeolites X, Y; zeolite ZSM-12; zeolite ZSM-5 or silicalite-1; zeolite Theta-1 or ZSM-22) and their micropore systems and dimensions (Weitkamp, 2000).

Because some of the $Si^{4+}$ is substituted by $Al^{3+}$, there is a net negative charge which is balanced by extra-framework exchangeable cations, mainly $Na^+$, $K^+$, $Ca^{2+}$ or $Mg^{2+}$. These cations are mobile and loosely held within the central cavities and surrounded by water molecules. The water molecules are loosely held in the pores and most zeolites can be reversibly dehydrated, and their cations are readily exchanged. This ion-exchange property accounts for the greatest volume use of zeolites today.

Figure 3.3 shows the structures of four selected zeolites along with their respective void systems and pore dimensions. In these commonly used representations, the T-atoms are located at the vertices, and the lines connecting them stand for T–O–T bonds.

The crystalline framework structure of zeolites contains voids and channels of discrete size. These may be divided into three major groups according to their pore/channel system. Table 3.1 presents a listing based on the largest pore opening.

Table 3.1. Classification of Zeolite Structure as a Function of the Number of $TO_4$ Units That Shape the Pore Opening (Schwarz et al, 1995).

| **8 Ring** | **10 Ring** | **12 Ring** |
|---|---|---|
| Bikitaite | Dachiardite | Beta |
| Brewsterite | Epistilbite | Cancrinite |
| Chabazite | Laumontite | Faujasite (Type X,Y) |
| Edingtonite | Stilbite | Gmelinite |
| Gismondine | ZSM-5 (silicalite) | Mazzite |
| Heulandite | ZSM-11 | Mordenite |
| Levyne | ZSM-22 (theta-1) | Offretite |
| Merlionite | ZSM-23 | Omega |
| Natrolite | ZSM-48 (Eu-2) | Type L |
| Paulingite | ZSM-50 (Eu-1) | ZSM-12 |
| Phillipsite | | |
| Rho | | |
| Thomsonite | | |
| TMA-E (AB) | | |
| Type A, ZK-5 | | |
| Yugawaralite | | |

The pore size is the two-dimensional opening of the zeolite and is determined by the number of tetrahedral atoms joined together. The structure is built up further by connecting the tetrahedral atoms in a three-dimensional array. This array can lead to larger inner cavities connected by pore openings. In some zeolites, there are no cavities, but a series of one-, two-, or three-dimensional channels through the structure.

### 3.2.1. Zeolite Acidity

The composition and structure of the centers responsible for the electron acceptor ability of zeolites are still subject to controversy and debate. Understanding the nature of these sites may provide control over their population and strength and make it possible to "tune" zeolites to produce optimal yields of radical cations. These features have obvious implications in the area of catalysis, especially for cracking and refining in the petrochemical industry.

Protons contained within the zeolite lattice are Brønsted sites. The unique environment of the Brønsted acidic protons in the micropores of zeolites controls the overall catalytic behaviour of zeolites to a significant extent (van Santen et al, 1995). The $H^+$ forms of zeolites can be prepared from alkali ion containing forms by ion exchange with concentrated hydrochloric acid at elevated temperatures. A milder method employs exchange of alkali ions by $NH_4^+$; thermal decomposition eliminates $NH_3$, leaving $H^+$ in the framework. The protons of acidic zeolites are covalently bonded to the oxygen closest to a negatively charged aluminum, forming oxonium species;

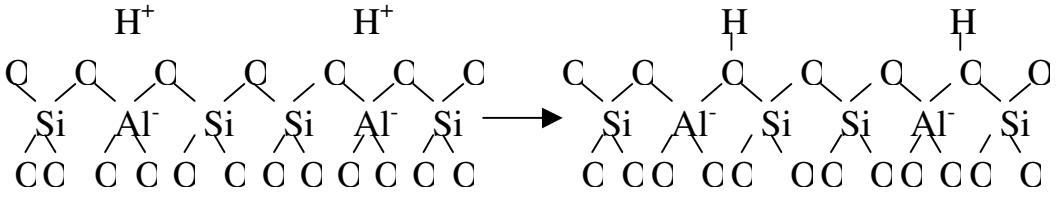


The bridging Si-(OH)-Al hydroxy groups can be monitored by IR spectroscopy (3800-3400 $cm^{-1}$).

Zeolites encompass sites with a wide range of acidities, whose distribution depends on their chemical composition and crystal structure. The acidity of hydroxy

groups in the framework decreases as the number of Al centers in the second coordination sphere increases.

Zeolites also contain Lewis sites; these were attributed to tricoordinated Al centers. Samples exhibiting Lewis acidity have octahedrally coordinated Al centers, suggesting that extraframework Al species (EFAl), generated during steaming or calcination of hydrated zeolites, are responsible for the Lewis acidity:

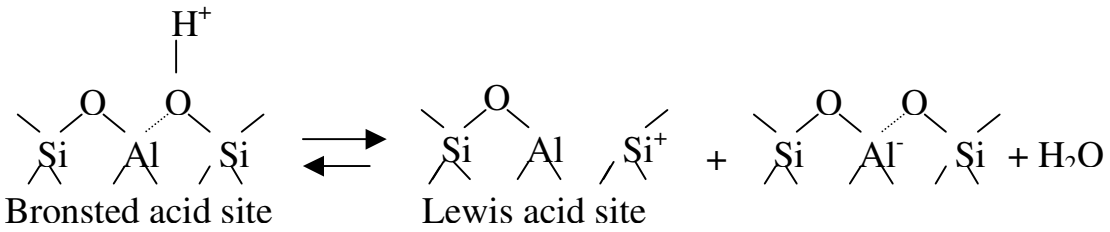


A variety of physicochemical techniques have been developed for the characterization of type, strength and numbers of acid sites on solid acid catalysts. Experimental methods used in the investigation of zeolite acidity are (Farneth et al,1995);

1) IR Spectroscopy
2) Temperature-Programmed Desorption of Amines
3) Alkane Cracking
4) UV-Visible Spectroscopy
5) Microcalorimetry
6) Solid-State NMR Spectroscopy

Temperature programmed desorption along with Fourier Transform Infrared (FTIR) spectroscopy has been used to study the acid sites in zeolite catalysts (Robb et al, 1998; Mukti et al, 2002; Selli et al, 1999).

The pyridine adsorption/desorption method specifically probes acid sites in solids by IR. In silica-alumina catalysts, pyridine complexed to Brønsted sites produces bands at 3260 $cm^{-1}$ and 3188 $cm^{-1}$ which are due to the $NH^+$ stretching vibrations and by bands at 1638 $cm^{-1}$ and 1545 $cm^{-1}$ as a result of the combined C-C stretching and in-plane CH and NH bending modes. Pyridine complexed to Lewis sites produces bands at 1452 $cm^{-1}$ and 1577 $cm^{-1}$ due to the combined C-C stretching and in-plane CH bending

modes. And bands at 1492 $cm^{-1}$ assigned to pyridine associated with Brønsted and Lewis sites. Other bands that form as a result of the pyridine hydrogen bonding with the hydroxyl groups can be removed by prolonged heating at 150°C under a vacuum (Cook et al, 1961). In this method, pyridine vapour is adsorbed onto dehydrated zeolite at room temperature and desorbed at increasing temperatures (e.g., in the range $250 > T > 400$ °C) at reduced pressure ($10^{-2}$ Pa) over a period of several hours. The amount of pyridine desorbed at different temperatures indicates the strength of the sites. Molar absorptivity coefficients of the pyridine Brønsted and Lewis bands are known and allow IR intensities to be converted to concentrations of acid sites (mol per gram of solid). Zeolites probed under similar conditions can be rated on a quantitative acidity scale. Acid sites on the external surface of pentasil zeolites can be probed by adsorbing a bulky base, such as 2,4-di-*tert*-butylpyridine.

With the possible exception of IR of adsorbed pyridine, temperature-programmed desorption (TPD) of ammonia is probably the most widely used method for characterizing acidity in zeolites. There are many variations on the method, but it typically involves saturation of the surface with ammonia under some set of adsorption conditions, followed by linear ramping of the temperature of the sample in a flowing inert gas stream. Ammonia concentration in the effluent gas may be followed by absorption/titration or mass spectroscopy. Alternatively, the experiment may be carried out in a microbalance and changes in sample mass may be followed continuously. The amount of ammonia desorbing above some characteristic temperature is taken as the acid-site concentration, and the peak desorption temperatures have been used to calculate heats of adsorption (Farneth et al, 1995).

For ZSM-5, going back to the earliest applications of ammonia TPD, it has been able to provide useful information about preparation variables, like ion-exchange conditions and deammoniation conditions necessary to optimize acid site concentration. Caution must be used to ensure that “physically adsorbed” species are not counted along with the ammonium ion sites. Depending on experimental conditions, like sample bed depth, carrier gas dynamics, and temperature control, desorption from nonprotonic binding sites can take place over a wide temperature range, even at temperatures approaching 600 K, where Brønsted sites are normally assumed. Deconvoluting the desorption trace to obtain Brønsted site concentrations is generally a matter of careful experimental control, but may not be possible under all conditions (Farneth et al, 1995).

In this study, IR spectroscopy with pyridine adsorption/desorption method was used to determine the catalyst acidities.

### 3.2.2 Shape Selectivity

Zeolites have a 1, 2 or 3 directional pore structure with a well defined pore size which gives them the ability to act as efficient 'molecular sieves'. The zeolites ability to preferentially sieve molecules can be used in a more useful way. If a reactant is sterically unable to enter the zeolite pores, where the reaction takes place, then the product resulting from that reactant is also restricted. In the second case, if a product forms inside the zeolitic cavity but is unable to leave, again it is restricted.

The fact that the pores of zeolites and molecules interacting with the surface of zeolites have dimensions in the same order of magnitude, leads to unique effects in catalysis for which the generic term shape-selective catalysis is in use today. Shape-selective catalysis encompasses all effects in which the selectivity of the heterogeneously catalyzed reaction depends unambiguously on the pore width or pore architecture of the microporous catalyst (Weitkamp, 2000). Shape selectivity is one of the most important properties of zeolites in their application in the field of catalysis. This property is greatly related to the pore size of the zeolite. There different types of shape selectivities are observed over zeolites as shown in Figure 3.4:

1. Reactant selectivity occurs when some of the molecules are too large to diffuse through the catalyst pores.
2. Product selectivity occurs when some of the products formed within the pores are too bulky to diffuse out as observed products. The bulky molecules are either converted to less bulky molecules or to coke that eventually deactivates the catalyst.
3. Restricted transition state selectivity occurs when certain reactions are prevented because the corresponding transition state would require more space than available in the cavities or pores. Neither reactant nor product molecules are prevented from diffusing through the pores. Reactions requiring smaller transition states proceed unhindered.

REACTANT SELECTIVITY

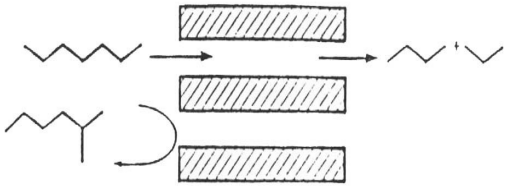

(i)

(ii)

(iii)

(iv)

(v) PRODUCT SELECTIVITY

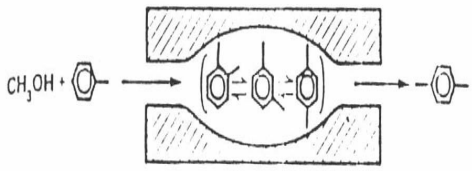


**(vi)**

**(vii)**

**(viii)**

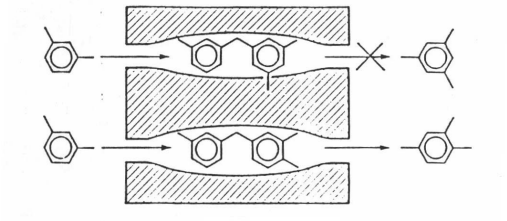

(ix)

(x) RESTRICTED TRANSITION

(xi) STATE SELECTIVITY

**(xii)**

**(xiii)**

Figure 3.4. Different types of shape selectivities of zeolites.

An example of the effect of shape selective catalysis is that that takes place in the Methanol to Gasoline (MTG) process developed by the Mobil Oil Company. A stream of gaseous methanol is passed over a H-ZSM-5 catalyst bed and a dehydration-polymerisation reaction takes place inside the pore. The resulting effect is a sharp cut off of product distribution at $C_{11}$ (gasoline) length fractions, the largest length of hydrocarbon that can fit inside the zeolite pore. A result of this cut-off is that no extra reprocessing is needed to remove heavier residues.

## 3.3. Zeolite Synthesis

Natural zeolites are found worldwide and were formed by igneous or sedimentary solution processes. But synthesizing a new or modified zeolite is a great challenge. It is possible to replicate all of the conditions except the time of formation, which is thousands of years in nature. Commercially, zeolites must be produced in hours or days; this, thus, requires optimizing the other variables to change the window of formation.

Progress in zeolite synthesis has been ongoing since commercial zeolites were first introduced 50 years ago. Most zeolites are made from the same reagents: alumina, alkali cations, and silica. Small variations in conditions can cause major differences in the structures that form.

The method of precipitation is the best known and most widely used procedure for synthesis of both monometallic and multimetallic oxides. Precipitation results in a new solid phase (precipitate) that is formed discontinuously (i.e., with phase separation) from a homogeneous liquid solution. A variety of procedures, such as addition of bases or acids, addition of complex-forming agents, and changes of temperature and solvents, might be used to form a precipitate.

The term coprecipitation is usually reserved for preparation of multicomponent precipitates, which often are the precursors of binary or multimetallic oxidic catalysts. The same term is sometimes improperly used for precipitation processes which are conducted in the presence of suspended solids.

Depending on the particular application, the newly formed solid phase may be further subjected to various treatments, such as aging and hydrothermal transformation, washing, filtration, drying, grinding, tableting, impregnation, mixing, and calcination. During all these preparative steps, physicochemical transformations occur which can profoundly affect the structure and composition of the catalyst surface and even its bulk composition.

The method of crystallization has found wide applications in the preparation of homogeneous microporous solids, a class of monophase crystalline solids in which the active phase is distributed uniformly. They comprise the general class of materials designated as molecular sieves.

When the crystal growth is carried out in aqueous solution above or near 375 K**,** the conditions are designated as “hydrothermal”; this has proven to be the most efficient way thus far to produce these microporous materials.

Many factors determine the type of synthetic zeolite produced. The thermodynamic variables include (Richardson, 1992, Weitkamp, 1998);

- composition of the gel,
- temperature and heat-up rate and,
- pressure.

The kinetic variables include;

- time of reaction;
- synthesis conditions (like order of mixing, gel aging, and stirring).

In addition to the thermodynamic and kinetic parameters some other factors also influence the nature and type of zeolite synthesized. These factors include;

- treatment of reactants prior to crystallization;
- the chemical and physical nature of the reactants ( such as silica and alumina sources);
- the influence of mineralizares;
- the templating effect of cations (typical cations include alkali metals, alkaline earth cations, $NH_4^+$, $H_3O^+$ ($H^+$), tetramethylammonium (TMA), other nitrogencontaining organic cations, rare earth ions, and noble metal ions) and
- additives.

Some zeolite properties that are determined during synthesis include:

- structure;
- silica-to-alumina ratio;
- pore size; and
- framework density (that is, atoms per unit cell).

A typical zeolite synthesis involves mixing together;

alkali,

sources of silica and alumina,

water, and

other components in appropriate proportions;

the resulting gel is then subjected to elevated temperatures. It is of interest to know what species are present at the beginning of the reaction. Aluminate solutions contain only

one type of ion at high pH; the tetrahedral $Al(OH)_4^-$ ion is the important species for normal zeolite synthesis. Silicate ions at high pH contain a range of small silicate polymers formed by corner-sharing tetrahedral $SiO_4$ units. Rings and cages are the preferred form of silicate species. Depending on the temperature and composition, the optimum crystallization time can range from several hours to several weeks. During this time period, the system is in a highly disordered state with a higher entropy than its ordered counterpart, the crystallized zeolite product. One can follow the course of a crystallization either by stopping the crystallization at various times and sampling the batch, by taking samples while the process is occurring, or by running the process in a series of identical crystallization vessels charged with the same batch of starting gel. The latter has been the most extensively used (Schwarz et al, 1995).

Inorganic cations present in the reaction mixture often appear as the dominant factor which controls the zeolite structure obtained; they can influence crystal morphology, crystallinity, and yield. The effect of the added cations is, indeed, complex and may be due to many factors. The presence of different cations (as well as amounts) will modify the pH of the mixture with crystallization time. Another possibility has been described as a template theory. An ion (or neutral species) is considered to be a template or crystal-directing agent if, upon its addition to the reaction mixture, crystallization is induced of a specific structure that would not have been formed in the absence of the template. The process has been analyzed as one in which the zeolite structure grows around the template; thus stabilizing certain pore structures or subunits. The theory is not only limited to explaining the effects of inorganic cations; it has been shown that neutral and ionic organic amines also follow a similar templating effect although other explanations have been suggested (Schwarz et al, 1995).

The water content of the starting mixture also plays an important role in determining the structure of the zeolitic product. Water has been proposed to interact strongly with cations present in solution and becomes itself a sort of template for structure control.

A schematic representation of synthesis of zeolites can be seen in Figure 3.5.

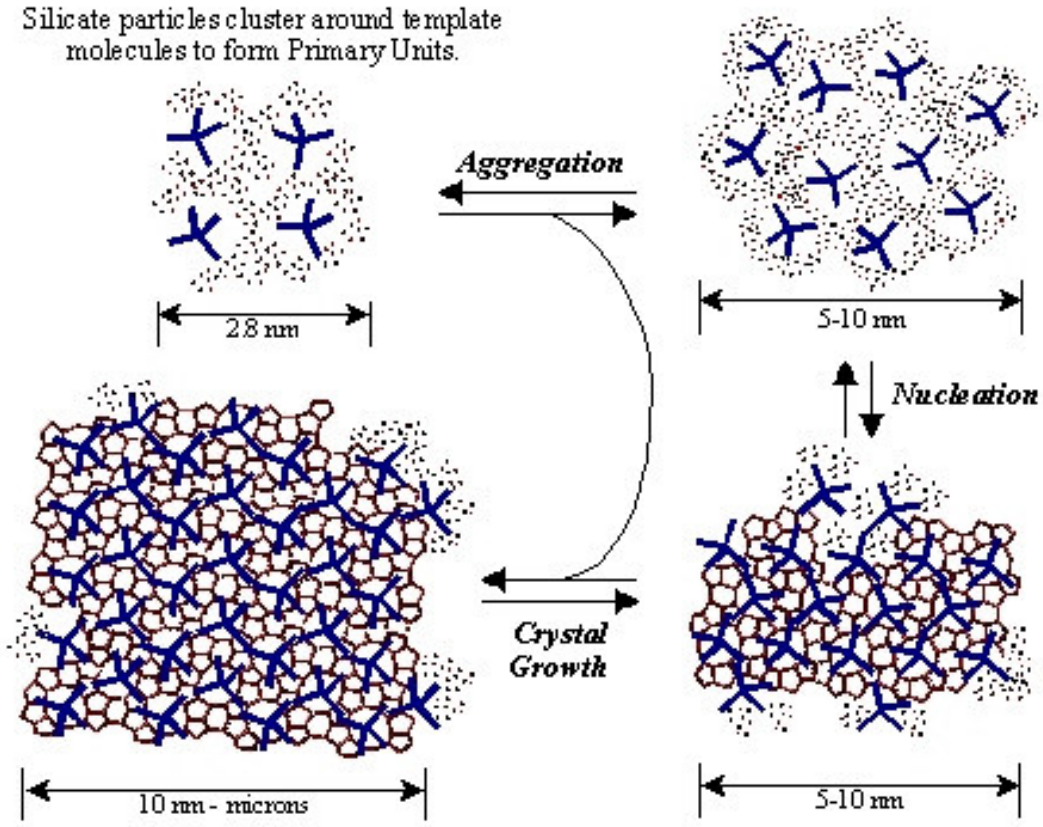


Figure 3.5. Schematic representation of synthesis of zeolites.

# CHAPTER 4

# EXPERIMENTAL STUDY

In this study, H-ZSM-5 synthesized, commercial H-ZSM-5 catalysts (received from Süd-Chemie, MFI-50 and MFI-90) and commercial $NH_4$-FER (received from Zeolyst, CP914c) zeolites were used. Synthesized ZSM-5, commercially supplied MFI-50 and MFI-90 were labelled as ZSM1-5, ZSM2-5 and ZSM3-5, respectively. For catalyst preparation these zeolites were modified by ion exchange with different metals which were Co, Ni, Cu and Zn, and by impregnation with Co. In addition, H-ZSM1-5 was ion exchanged with Mn and Mg metals. The catalysts were characterized and tested in n-butene skeletal isomerization reaction.

## 4.1. Synthesis of Na-ZSM1-5, Preparation of H-ZSM-5 and H-FER Zeolite Catalysts

The chemicals used for the preparation of the synthesis gel is given in Table 4.1.

Table 4.1. The chemicals used for the synthesis of ZSM1-5 zeolite samples.

| Chemicals | |
|---|---|
| Fumed Silica | Sigma, 99.8 % |
| Aluminium Hydroxide [$Al(OH)_3$] | Merck, pure powder |
| Sodium Hydroxide [NaOH] | Sigma, >98.4 % |
| Tetra-Propyl-Ammonium Bromide [TPABr] | Fluka, >98 % |

Na-ZSM-5 was synthesized, with an initial $SiO_2/Al_2O_3$ molar ratio of 30. The composition of the hydrogel was applied according to the method given in literature (Nicolaides, 1999). The detailed description of gel preparation is as follows:
Three different solutions named, A, B and C, were prepared;
Solution A: 20.10 g fumed silica was added to 162.50 ml deionised water.

Solution B: 4.48 g NaOH and 1.48 g $Al(OH)_3$ was dissolved in 18.75 ml deionised water. The solution B was added to the solution A and mixed for 15 minutes in order to obtain a homogeneous solution.
Solution C: 7.43 g of tetra-propyl-ammonium bromide (TPABr) was dissolved in 75 ml of water. Solution C was added to the homogeneous solution of A and B. After the addition of 110 ml deionised water, the mixture was agitated for 15 minutes. Then, the gel was transferred into an autoclave.

The initial composition of the gel prepared was:

12.84 $Na_2O$ : $Al_2O3$ : 30.28 $SiO_2$ : 6.4 TPABr : 3962.6 $H_2O$

This composition was determined on the basis of following postulated equations:

$2NaOH = Na_2O + H_2O$
$2Al(OH)_3 = Al_2O_3 + 3H_2O$

The autoclave was then put into a oven at 150 °C and kept for 96 hours. The reaction was performed under static conditions. At the end, the autoclave was taken out from the oven and cooled down by immersing into the cold water. The zeolite formed was filtered and continuously washed with excess amount of deionised water. The cake was allowed to dry at ambient conditions and then dried in an oven at 110 ºC for 24 hours. An air-ventilated and temperature-programmable furnace was used for the calcination of the dried zeolite. The temperature of the furnace was increased from room temperature to 300ºC (in about 30 minutes) and allowed to stay at this temperature for 30 minutes. After that, it was heated to 540 ºC with a heating rate of 3 ºC/min and kept at this temperature for 8 more hours. The temperature of the furnace was slowly cooled down to room temperature. Eventually, the organic template was removed and Na-ZSM-5 zeolite was obtained.

The synthesized Na-ZSM-5 were ion-exchanged with 1 M $NH_4Cl$ (Sigma-Aldrich, 99.5 %) solution for 48 hours at room temperature under continuos agitation. After ion exchange the zeolites were washed thoroughly with deionized water until they are free of chloride ions. Then, the samples were dried at 110 ºC for 24 hours. The dried

sample was calcined again. For this time the furnace was slowly heated to 540 ºC (3 ºC/min) and calcined for 4 hours to remove $NH_3$ and to obtain H-ZSM1-5.

The zeolites commercially supplied from Süd-Chemie were received in H form. These zeolites were directly used without the need of any pre-treatment.

However, ferrierite zeolites which were commercially supplied from Zeolyst were received in $NH_4$ form. They were calcined before modifications. The calcination was the same as used to calcine ZSM-5 catalysts. The furnace was slowly heated to 540 ºC (3 ºC/min) and kept for 4 hours to remove $NH_3$ and to obtain H-FER.

Table 4.2 shows the $SiO_2/Al_2O_3$ ratios of the commercially supplied zeolites.

Table 4.2. The $SiO_2/Al_2O_3$ ratios of the commercially supplied zeolites.

| **Zeolite** | **Company** | **$SiO_2/Al_2O_3$** |
|---|---|---|
| ZSM2-5 | Süd-Chemie | 50 |
| ZSM3-5 | Süd-Chemie | 90 |
| Ferrierite | Zeolyst | 20 |

Finally, the catalysts were pressed under 825 MPa pressure and then ground and sieved. In order to minimize internal diffusional limitations during the tests, the particles having sizes between 125-250 μm were taken and used in the reaction as catalysts (Byggningsbacka et al. 1998).

## 4.2. Modification of Catalysts

### 4.2.1. Ion Exchange

The list of the chemicals used for ion exchange is given in Table 4.3. The chemicals were used without further purification.

For ion exchange one of the metal salt given in Table 4.3 was dissolved in deionized water. Zeolite catalyst was then added into this metal solution. The solid to liquid ratio was 1 g zeolite: 100 ml metal solution. The prepared slurries were kept at 80 °C for 4 hours using a water bath equipped with a shaker (180 rpm). Following the ion exchange process, the slurry was filtered and washed with deionized water in order to

remove excessive metal ions. The samples then were dried at 110 °C over night and calcined at 500 °C for 4 hours.

Table 4.3. The chemicals used for ion exchange.

| Chemicals | |
|---|---|
| Cobalt (II) Nitrate Hexahydrate ($Co(NO_3)_2.6H_2O$) | Sigma, 98.3 % |
| Nickel (II) Nitrate Hexahydrate ($Ni(NO_3)_2.6H_20$) | Sigma, 99.0 % |
| Zinc Nitrate Hexahydrate ($Zn(NO_3)_2.6H_20$) | Fluka, >99.0 % |
| Cupric Nitrate ($Cu(NO_3)_2.2H_2O$) | Sigma, 99.0 % |
| Magnesium Nitrate-6-Hydrate | Riedel-de Haën, 97 % |
| Manganese (II) Nitrate Hydrate | Aldrich, 98 % |

In order to see the effect of the amount of metal loading, different metal amounts were loaded onto synthesized H-ZSM1-5 using various $Co(NO_3)_2$ metal solutions. Zeolites were treated with a series of $Co(NO_3)_2$ solutions of initial concentrations 0.001 M, 0.005 M, 0.01 M and 0.02 M.

After the activity tests, it was decided to work with initial concentration of 0,01 M for each metal at 80 °C for 24 hours using a water bath equipped with a shaker. The concentrations of different metal solutions used for ion exchange are given in Table 4.4.

Table 4.4. The initial concentrations of different metal salt solutions.

| Metal | Initial Concentration |
|---|---|
| $Co(NO_3)_2$ | 0.001 M, 0.005 M, 0.01 M, 0.02 M |
| $Ni(NO_3)_2$ | 0.01 M |
| $Zn(NO_3)_2$ | 0.01 M |
| $Cu(NO_3)_2$ | 0.01 M |
| $Mg(NO_3)_2$ | 0.01 M* |
| $Mn(NO_3)_2$ | 0.01 M* |

(*: only studied with H-ZSM1-5)

### 4.2.2. Impregnation

Impregnation test was made only for $Co(NO_3)_2$. The preparations of Co impregnated catalysts were carried out by incipient wetness method. Appropriately weighed quantities of cobalt nitrate were taken with the desired catalyst so that the total metal content in the catalyst was around 1.5 % by weight. The amount of solutions needed were calculated by using the pore volume of the catalysts. The aqueous solution of the cobalt precursor was slowly added to the support at room temperature. Then, kept for 4 hours in room temperature. Next, the solid was dried at 100 °C for 24 hours and calcined at 500 °C for 4 hours.

## 4.3. Characterization of the Catalysts

The metal loadings of the catalysts were determined by Varian-96 Inductively Coupled Plasma Atomic Emission Spectrometer (ICP-AES) with fusion dissolution method. The method can be summarised as:
0.2 g of sample was mixed with 2 g of lithium tetraborate, then mixture was fused in furnace at 1000 °C for 1 hour and allowed to cool. Formed glass bead was dissolved in 1.6 M $HNO_3$ solution on a magnetic stirrer. Solution was completed to 250 ml and diluted if necessary.

The $SiO_2/Al_2O_3$ ratio for each sample was calculated using Energy Dispersive X-Ray System (EDX) attached to the SEM.

IR characterizations were carried out between 400 and 4000 $cm^{-1}$ with Shimadzu FTIR-8201 model Fourier Transformed Infra-red Spectrometer using KBr pellet technique. KBr pellets were prepared by pressing a mixture of 6 mg catalyst sample and 200 mg KBr.

The crystalline structures of the samples were determined by Philips X'Pert diffractometer with CuKα radiation. The scattering angle 2θ was varied from 5 °C to 40 °C, with a step length of 0.02.

The morphology of the samples were investigated by Philips SFEG 30S scanning electron microscopy (SEM).

Nitrogen physisorption studies were performed using Micromeritics ASAP 2010 model static volumetric adsorption instrument. The samples were dried in oven at

100°C over night prior to degassing. Prior to adsorption experiments, the zeolites were outgased at 300 °C for 24 hours under 5 μmHg vacuum.

The acidity measurements of the catalysts were made by IR spectroscopy with pyridine adsorption/desorption method. The samples were activated at 300 ºC under $N_2$ flow for 1 hour and then under vacuum ($2 \times 10^{-2}$ mmHg) for 1 h. Adsorption of pyridine was carried out at 150 ºC for 30 minutes. Before FTIR analysis the samples were kept 150 °C under $N_2$ flow at 1 h and then under vacuum ($2 \times 10^{-2}$ mmHg) for 1 hour in order to desorb the physisorbed pyridine.

## 4.4. Catalyst Testing

A fixed bed reactor system illustrated in Figure 4.1. was used for the testing of catalysts for 1-butene skeletal isomerization reaction and pyridine adsorption experiments. The reaction system was composed of a quartz fixed bed tubular reactor (10 mm in diameter and 65 cm in length) heated with a tubular furnace. The reactant 1-butene and the dilutant nitrogen were mixed and then fed to the reactor. Their flow was set and controlled by mass flow controllers.

The loading of the catalyst to the reactor was done as follows: initially a proper amount of quartz wool was placed inside the quartz reactor. On top of it, successively, 0.2 g of quartz sand, 0.05 g catalysts and another 0.2 g of quartz sand was loaded. Thus, the catalyst was placed between two layers of quartz sands. After loading, the reactor was inserted inside the tubular furnace. Swagelock ultra torr fittings and bored through connectors were used for the leak free connection of the quartz reactor and the thermocouple.

Before the reaction test started, the catalyst was heated to 440 ºC in 60 minutes under 100 ml/min flow of nitrogen (99.99 %) and maintained for additional 45 minutes at this temperature for activation and then cooled down to 375 ºC, which was the reaction temperature. The reaction was started by flowing 1-butene (98 %, 8 ml/min) and nitrogen (100 ml/min) mixture to the reactor. This gives 7.27 % 1-butene in the reactor feed gas.

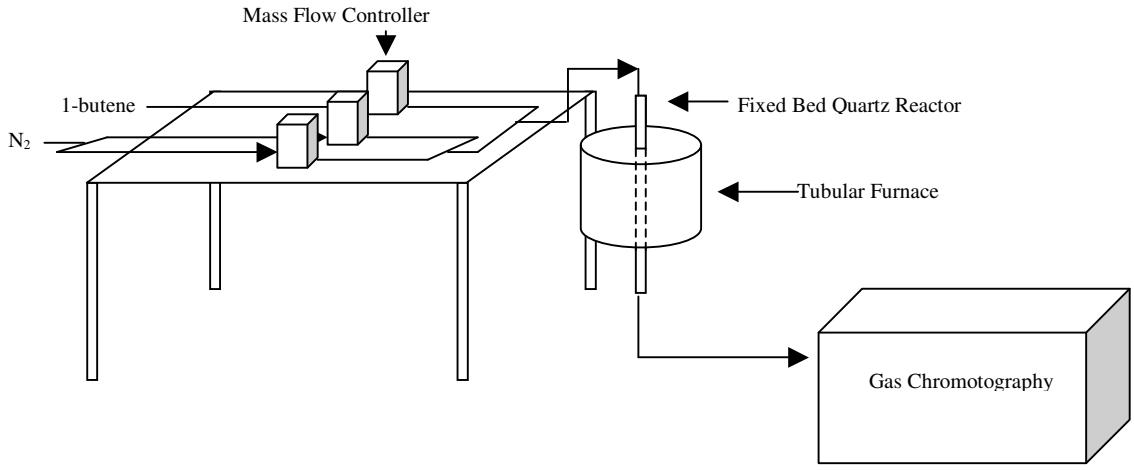


Figure 4.1. The experimental set-up used for catalyst testings and pyridine adsorption experiments.

The reactor effluent was connected to the sampling loop system of Gas Chromatography (Agilent Technologies 6890N Network GC System) for online gas analysis. The line from the reactor outlet to the GC was externally heated and isolated in order to prevent condensation. At time intervals product sample was analyzed. The online gas chromatograph was equipped with a Flame Ionization Detector (FID) and a fumed silica KCl column (GSAlumina KCl, 50 m × 0.53 mm). Helium was used as carrier gas with a flow of 6.1 ml/min and 47.4 kPa. A stepped heating and flow program was applied to the GC column for fine separation of all the reaction products. The temperature program used included the following steps:

(1) heating from 50°C to 100°C at 5 °C/min.

(2) heating from 100°C to 180°C at 40 °C/min and

(3) holding at 180 °C for 15 min.

# CHAPTER 5

# RESULTS AND DISCUSSION

## 5.1. Characterization of the Catalysts

### 5.1.1. ZSM-5

#### 5.1.1.1. ZSM1-5

The ion exchanged samples were labelled as M-ZSM1-5 where M indicates the metal ion used. The impregnated samples labelled as ImpZSM1-5. The XRD patterns of the ZSM1-5 samples prepared with different metals and methods are given in Figure 5.1.

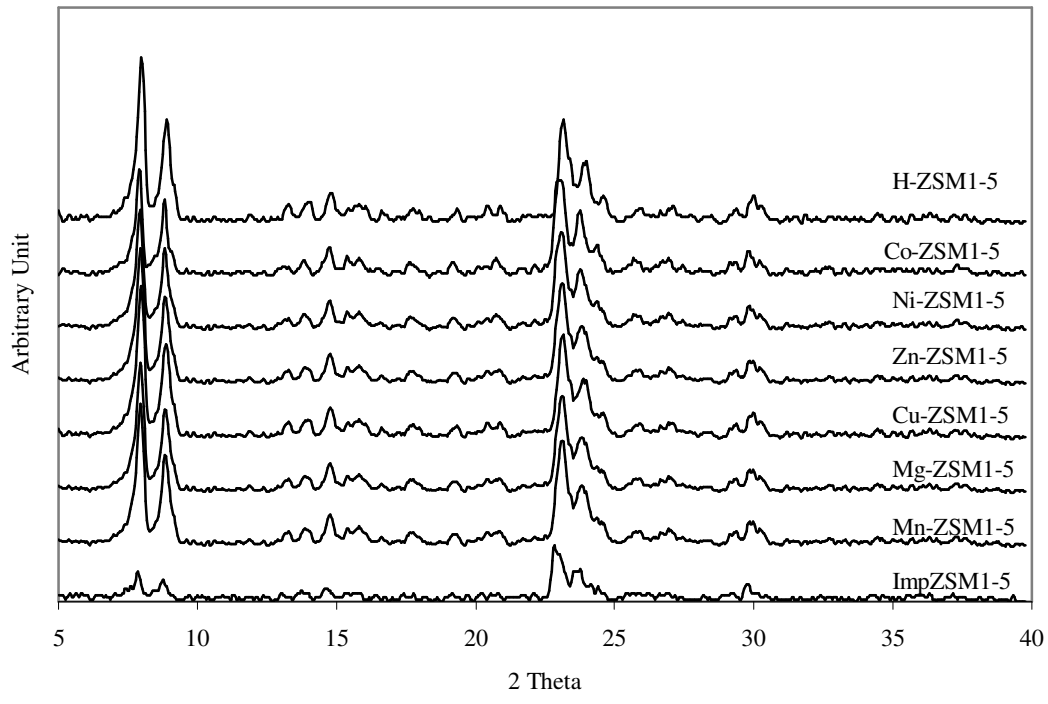


Figure 5.1. XRD patterns of synthesized ZSM1-5 samples prepared with different metals and methods.

The positions of all peaks of the ZSM1-5 samples were the same and in accordance with those found in literature for the ZSM-5 structure (Kumar, 1996). The XRD patterns of ion exchanged samples were similar to the H-ZSM1-5 zeolite. This indicated that ion exchange did not affected crystal structure of the H-ZSM1-5 zeolite.

The peaks indicate that the crystallinity of the zeolite support was not highly affected by ion exchange method. Also, since MFI peak at $2\theta = 23°$ is unchanged, no dealumination occurs during either of the modification methods. However, on impregnation, the intensities of the peaks at $2\theta = 7.9°$ and 8.5° decreased in comparison to those for H-ZSM1-5. This decrease indicates the presence of inorganic material in the intracrystalline voids. This fact could also be inferred from the decreasing surface areas of the impregnated samples relative to those of the ion exchanged samples, as discussed later.

Figure 5.2 shows ion exchanged ZSM1-5 samples prepared with different Co loadings. The crystallinity of the H-ZSM1-5 was not affected with the increase in the metal loading to the zeolite support.

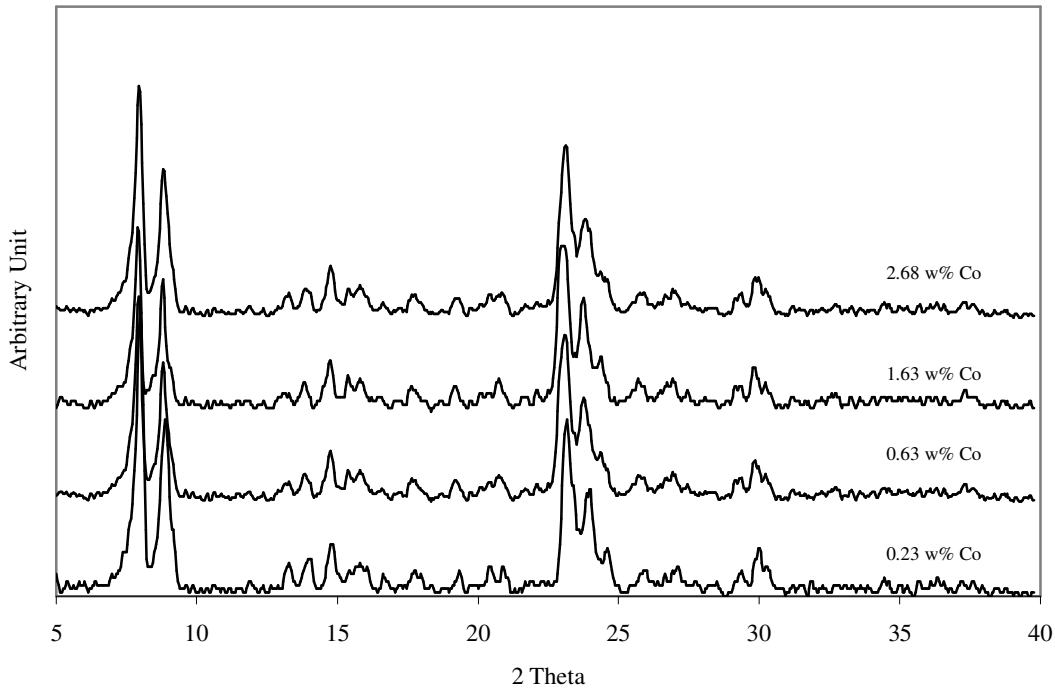


Figure 5.2. XRD patterns of ZSM1-5 samples prepared with different Co loadings.

Typical SEM images of the parent, Co and Cu ion exchanged and Co impregnated samples are given in Figure 5.3. Spherical crystals were observed. Similar SEM images were obtained for ion exchanged catalysts. This also confirms the XRD findings that the crystal structure of the catalysts were not affected by ion exchange. They all showed clean surface zeolite crystals. However, with the impregnated sample a clear difference was observed. There were some small particles distributed over the zeolite surface of the impregnated catalyst. These particles probably indicate the agglomerates of cobalt particles. Also, in the literature similar observations were made by H-ZSM-5 impregnated with nickel oxide. These deposits on the surface of the zeolite

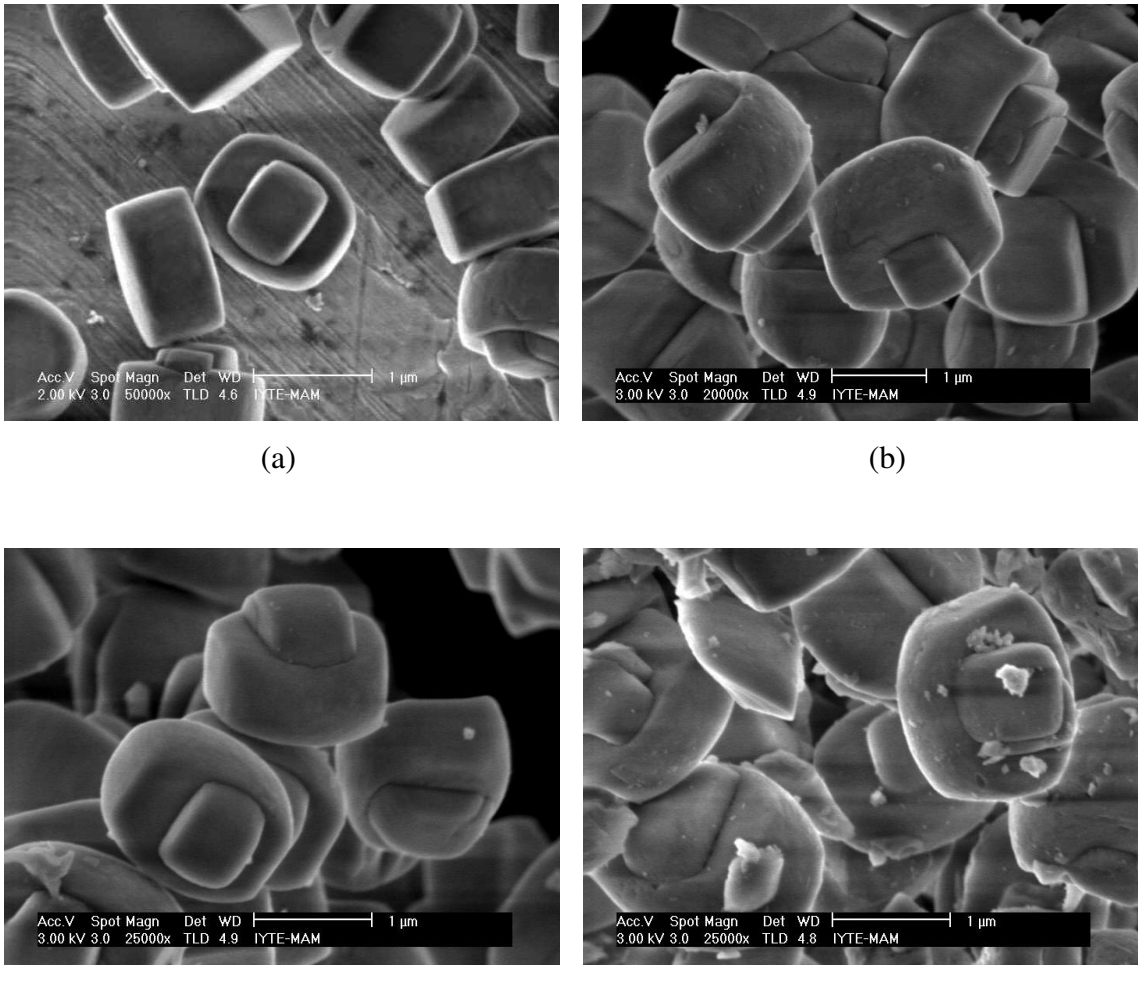


Figure 5.3. SEM images of ZSM1-5 and some modified samples (a: HZSM1-5, b: 1.45 w% Co, c: 1.57 w% Cu, d: ImpZSM1-5).

were attributed to nickel oxide particles (Romero et al, 1997). The SEM images showed that crystallite size of different ZSM1-5 samples was almost uniform and around 1.4 μm.

The textural properties and metal loadings for the ZSM1-5 catalysts were presented in Table 5.1. The BET surface area of the catalysts changed between 436.42-411.49 $m^2/g$. The catalysts were found to have very high surface area which is typical for a well crystalline MFI structure. Pore volume and median pore diameters for the catalysts were calculated using Howarth-Kowazoe method. Pore diameters and pore volumes of the catalysts decreased with metal loading. They varied with the metal type. Considering Co-ZSM-5 samples, it's seen that, increasing the metal loadings of the catalysts decreased the surface area. The surface area decreased slightly by ion exchange, up to 5 %. The highest decreases were observed with Cu, Mn and Mg ion exchanged catalysts. The lowest surface area was obtained from cobalt impregnated ZSM1-5. This indicated that some of the pores were closed by impregnation. Srinivas et al (2002), impregnated cobalt nitrate to give 5 w% metal loading. Their results also showed that impregnation with the metal lowered the surface area of the zeolite.

Table 5.1. Textural properties and metal loadings for the ZSM1-5 samples.

| Sample | Metal Loading (w%) | BET Surface Area ($m^2/g$) | H.K. Pore volume ($cm^3/g$) | H.K. Median Pore Diameter (Å) |
|---|---|---|---|---|
| H-ZSM1-5 | | 436.42 | 0.215 | 9.3 |
| Co-ZSM1-5 | 2.89 | 419.55 | 0.183 | 8.3 |
| | 1.45 | 425.76 | 0.207 | 7.8 |
| | 0.63 | 422.57 | 0.201 | 8 |
| | 0.23 | 423.69 | 0.205 | 7.9 |
| Ni-ZSM1-5 | 1.37 | 421.88 | 0.196 | 8.1 |
| Zn-ZSM1-5 | 1.52 | 422.71 | 0.189 | 8.3 |
| Cu-ZSM1-5 | 1.57 | 417.89 | 0.209 | 9 |
| Mn-ZSM1-5 | 1.38 | 416.36 | 0.169 | 7.4 |
| Mg-ZSM1-5 | 1.47 | 417.45 | 0.18 | 8.7 |
| ImpZSM1-5 | 2.22 | 411.49 | 0.175 | 5.7 |

The chemical composition of the parent ZSM1-5 catalyst determined was given in Table 5.2. The $SiO_2$ /$Al_2O_3$ ratio of the catalyst was calculated as 29.6.

Table 5.2. Chemical composition of the parent ZSM1-5 catalyst.

| **Component** | **Mol %** |
|---|---|
| $SiO_2$ | 93.6±1.4 |
| $Al_2O_3$ | 3.1±0.6 |
| $SiO_2$ /$Al_2O_3$ | 29.6 |

## 5.1.1.2. ZSM2-5

The ion exchanged sampled were labelled as M-ZSM2-50 where M indicates the metal ion used. The impregnated sample was labelled as ImpZSM2-5. The XRD patterns of the prepared samples are given in Figure 5.4.

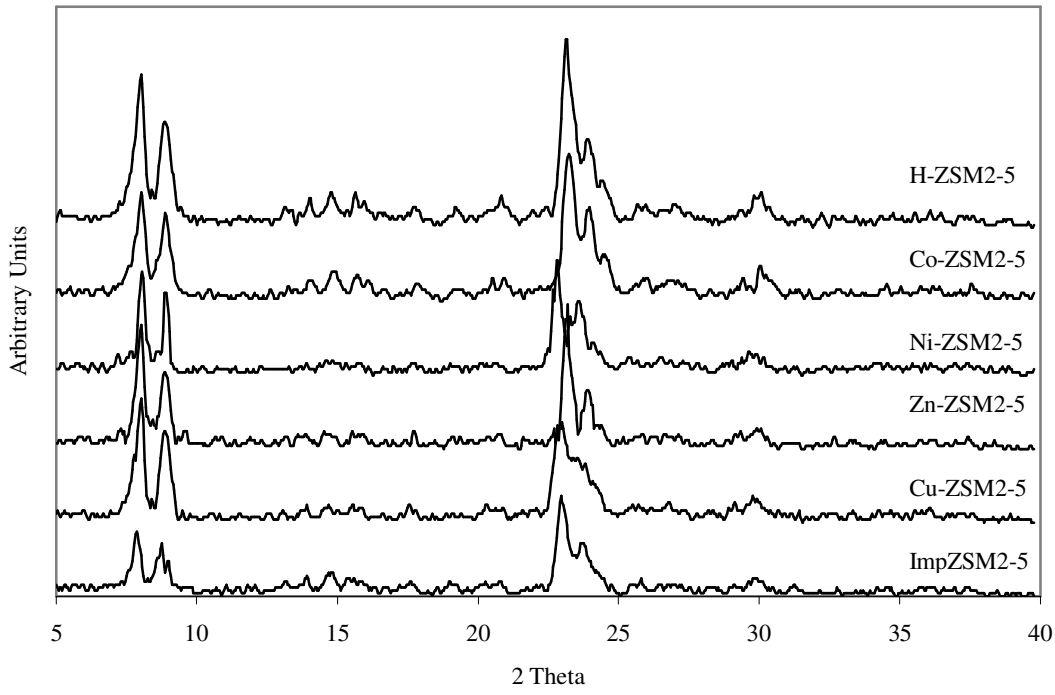


Figure 5.4. XRD patterns of H-ZSM2-5 and its modified samples.

The XRD patterns of ZSM2-5 samples were in accordance with those found in literature for the ZSM-5 structure. The similar XRD patterns of ion exchanged samples with the parent ZSM2-5 zeolite indicates that the ion exchange did not affected crystal structure of the H-ZSM2-5 zeolite. However, when the zeolite was impregnated with Co, the intensities of the peaks at $2\theta$ = 7.9° and 8.5° decreased in comparison to those for H-ZSM2-5.

In Figure 5.5 SEM images of the parent, Co and Zn ion exchanged and Co impregnated samples are given. The morphologies of this zeolite is very different that of synthesized ZSM-5 zeolite. It has a sponge like morphology with crystals smaller than 100 nm.

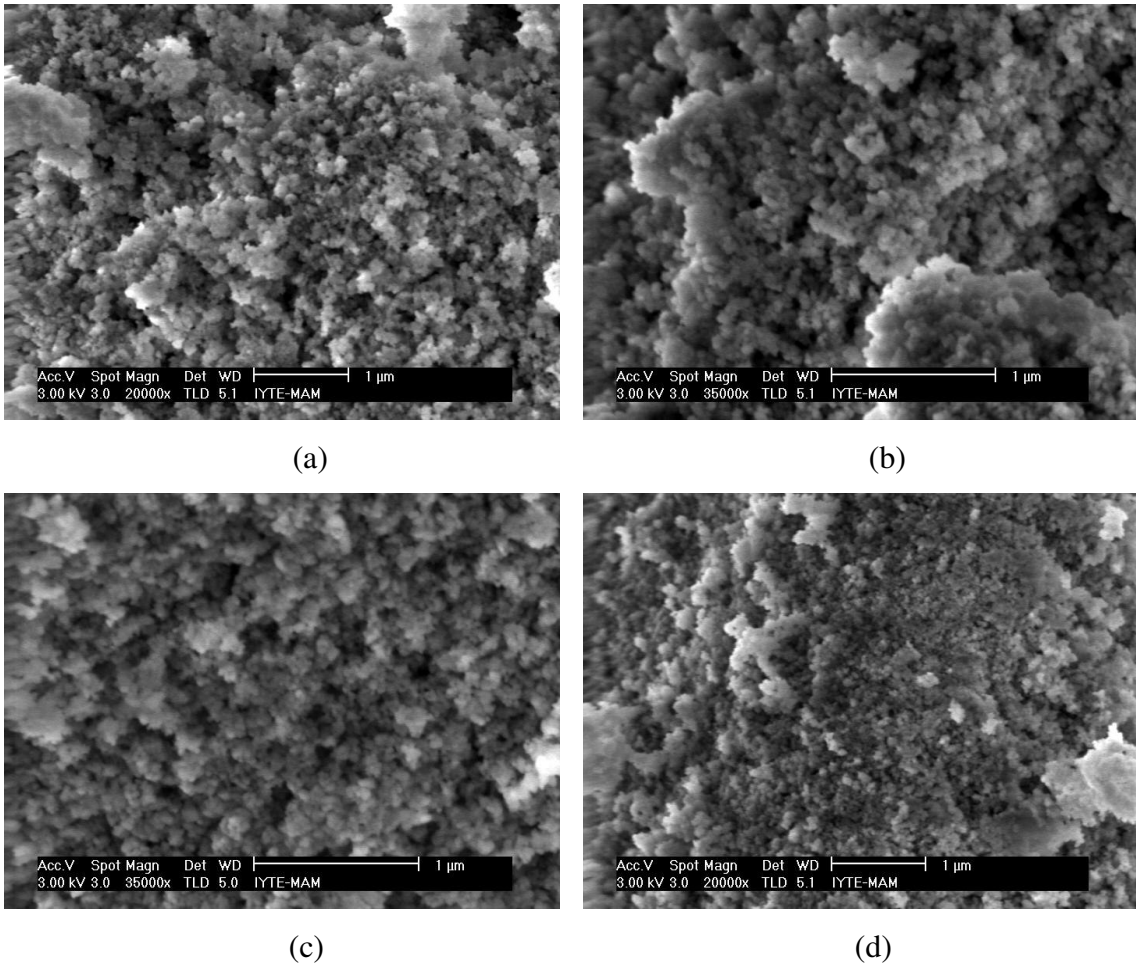


(a) (b)

(c) (d)

Figure 5.5. SEM images of H-ZSM2-5 and some of its modified samples (a: H-ZSM2-5, b: Co-ZSM2-5, c: Zn-ZSM2-5, d: ImpZSM2-5).

Table 5.3 presents the results of metal loadings and surface area with BET method, pore volume and median pore diameter measurements with Hovarth-Kowazoe method of the six ZSM2-5 catalyst samples. The catalysts were found to have different surface areas. The total BET surface areas for these samples range from 394.78 to 460.49 $m^2/g$. The surface area decreased with ion exchange, up to 13%, except with Co. Co ion exchanged catalyst had a similar surface area with the parent catalyst. The highest decrease was observed with Zn. Also, pore diameter and pore volume of the catalysts decreased with metal loading. These catalysts had pore sizes between 5.3 and 5.9 Å, which are much lower than ZSM1-5 catalysts (between 7.4 and 9.3 Å). Impregnation with Co decreased the surface area, pore diameter and pore volume of the catalyst.

Table 5.3. Textural properties and metal loadings of the ZSM2-5 samples.

| Sample | Metal Loading (w%) | BET Surface Area ($m^2/g$) | H.K. Pore volume ($cm^3/g$) | H.K. Median Pore Diameter (Å) |
|---|---|---|---|---|
| H-ZSM2-5 | | 455.7 | 0.21 | 5.9 |
| Co-ZSM2-5 | 1.12 | 460.49 | 0.209 | 5.7 |
| Ni-ZSM2-5 | 1.33 | 414.49 | 0.196 | 5.8 |
| Zn-ZSM2-5 | 1.42 | 394.78 | 0.185 | 5.6 |
| Cu-ZSM2-5 | 1.35 | 447.62 | 0.189 | 5.7 |
| ImpZSM2-5 | 1.78 | 429.57 | 0.172 | 5.3 |

Table 5.4 presents the chemical composition of the parent ZSM2-5 catalyst. The $SiO_2$ /$Al_2O_3$ ratio of the catalyst determined was lower than that is reported by the manufacturer. It was calculated as 44.7.

Table 5.4. Chemical composition of the parent ZSM2-5 catalyst.

| **Component** | **Mol %** |
|---|---|
| $SiO_2$ | 93.8±2.5 |
| $Al_2O_3$ | 2.1±1 |
| $SiO_2$ /$Al_2O_3$ | 44.7 |

The acidity of the catalysts determined by pyridine adsorption are given in Figure 5.6. It was observed from each spectrum that the zeolite in its metal loaded and H form had Brønsted and Lewis acid sites. From the spectra, it can be observed that the ZSM2-5 catalysts did not present the band at 1455 $cm^{-1}$ which is related to Lewis acidity. Houzvicka et al (1996) demonstrated that isomerization of linear butene is catalyzed by Brønsted acid sites. It was also shown that Lewis acid sites do not have a significant influence on the selective reaction. There is a broad band at 1548 $cm^{-1}$ which is assigned to Brønsted acid sites. The intense band at 1490 $cm^{-1}$ assigned to Brønsted and Lewis acid sites.

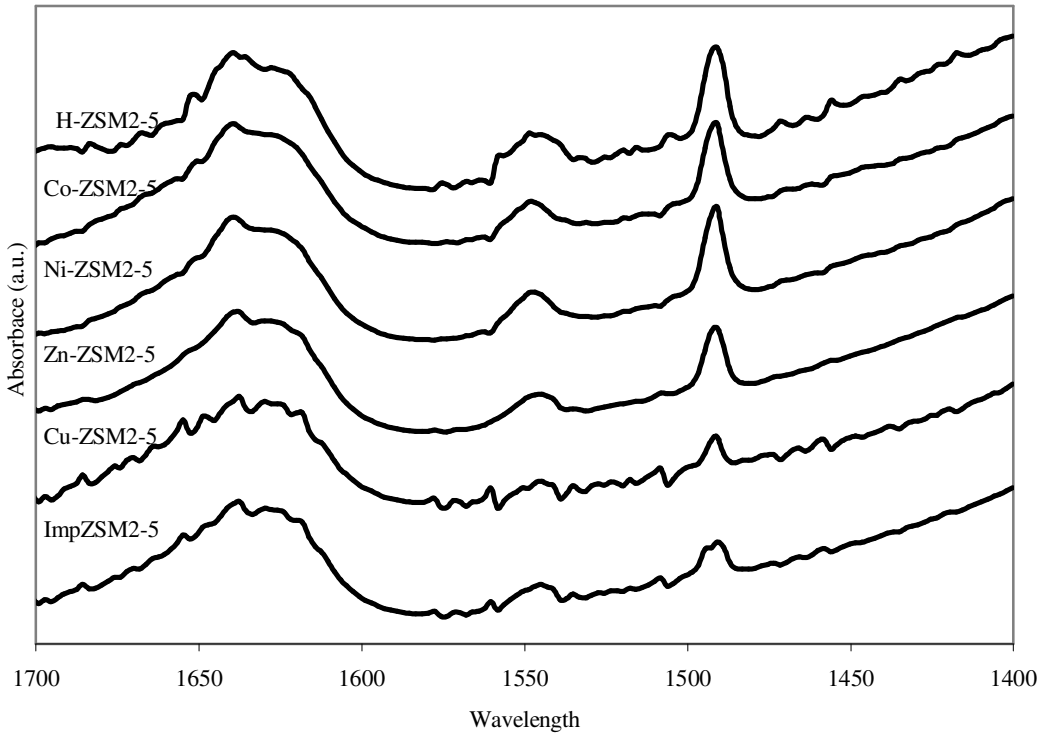


Figure 5.6. IR spectra of pyridine adsorbed metal loaded ZSM2-5 zeolites.

Acidities of the zeolites varied with the type of the metal loading. H-ZSM2-5 showed the highest acidity when compared to other modified samples. Cobalt impregnated Imp-ZSM2-5 showed the lowest acidity. The acidities of the modified ZSM2-5 zeolites, even though some of them very close to each other, decreased with the following order; H-ZSM2-5 > Co-ZSM2-5 > Ni-ZSM2-5 > Zn-ZSM2-5 > Cu-ZSM2-5 > ImpZSM2-5.

### 5.1.3. ZSM3-5

The ion exchanged sampled labelled as M-ZSM3-5 where M indicates the metal ion used. The impregnated sample was labelled as ImpZSM3-5. The XRD patterns of the catalysts are given in Figure 5.7. It was found that crystallinity of H-ZSM3-5 was not effected by ion exchange with different metals, as observed with other ion exchanged ZSM-5 catalysts studied. The intensities of the major peaks ($2\theta$ = 7.9, 8.5 and 23°) reduced by impregnation. This showed that some intracrystalline pores were filled with Co.

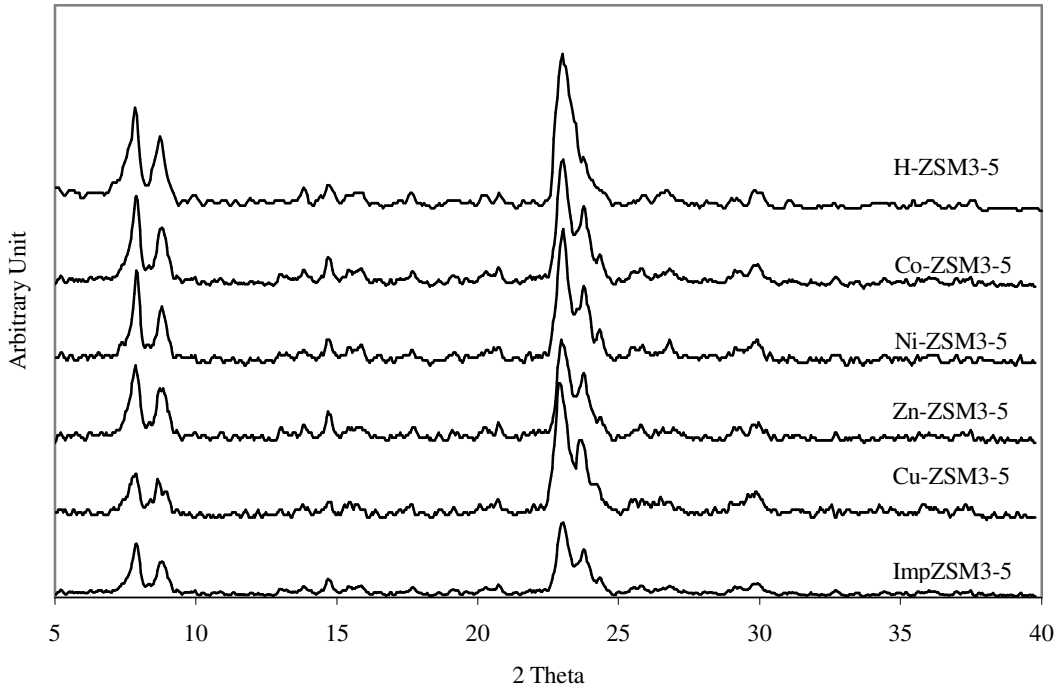


Figure 5.7. XRD patterns of H-ZSM3-5 and its modified samples.

The morphology of some M-ZSM3-5 catalysts are presented in Figure 5.8. Any major difference was not observed between the samples. The samples showed similar appearance and particle size with ZSM2-5. The particle size was found to be very small when compared to H-ZSM1-5.

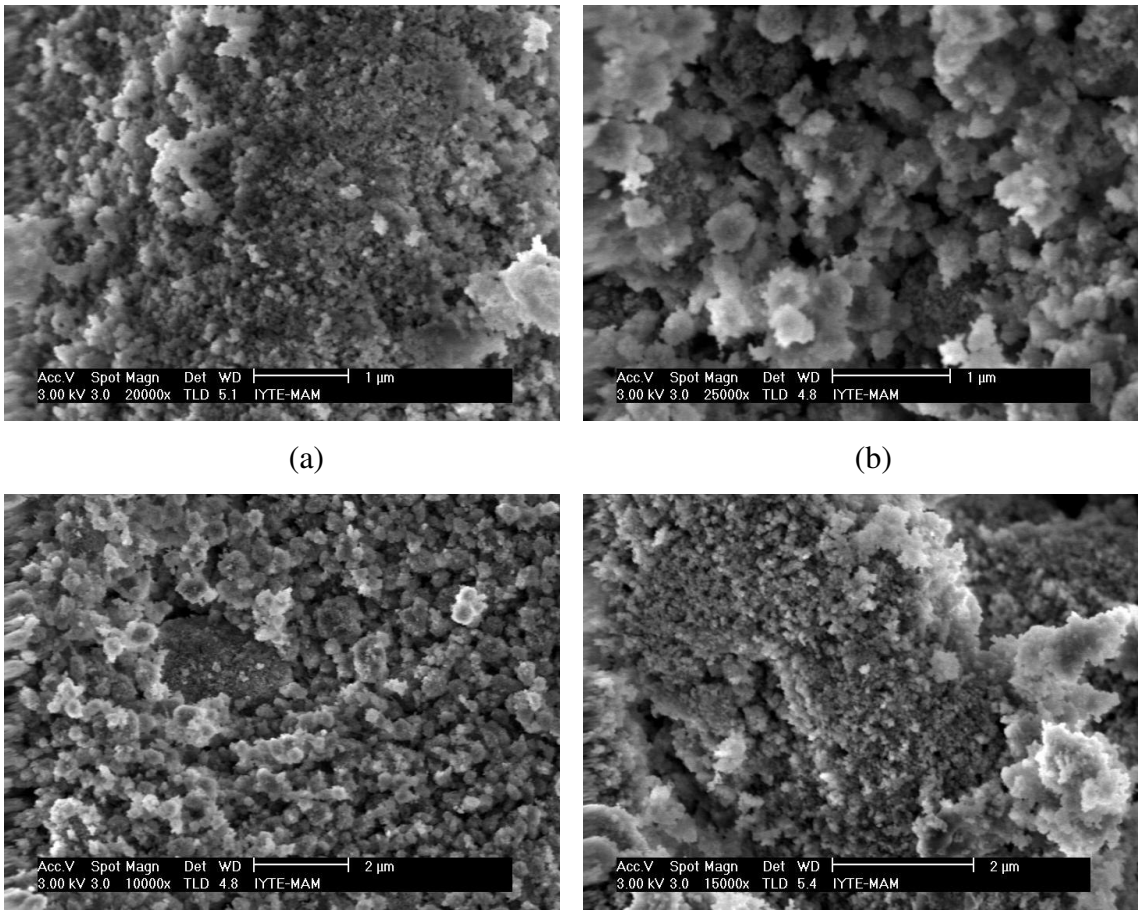


Figure 5.8. SEM images of H-ZSM3-5 and some of its modified samples (a: H-ZSM3-5, b: Co-ZSM3-5, c: Ni-ZSM3-5, d: ImpZSM3-5).

The specific surface areas of the samples were calculated by using the BET Method, the pore diameters and pore volumes were calculated by using Hovarth-Kowazoe Method and the results are presented in Table 5.5. The total BET surface areas of the catalysts prepared by ion exchange was close to the parent zeolite. However, the catalysts prepared by impregnation had lower surface area (decreased by ~5%). The catalysts had pore sizes between 5.4 and 5.9 Å. This pore size is close to the pore sizes for ZSM-5 zeolites. The lowest pore size was obtained for the catalyst prepared by impregnation. This could be due to the blockage of pore upon impregnation.

Table 5.5. Textural properties and metal loadings of the ZSM3-5 samples.

| Sample | Metal Loading (w%) | BET Surface Area ($m^2/g$) | H.K. Pore volume ($cm^3/g$) | H.K. Median Pore Diameter (Å) |
|---|---|---|---|---|
| H-ZSM3-5 | | 446.97 | 0.203 | 5.8 |
| Co-ZSM3-5 | 1.32 | 442.88 | 0.201 | 5.9 |
| Ni-ZSM3-5 | 1.23 | 439.57 | 0.195 | 5.9 |
| Zn-ZSM3-5 | 1.52 | 436.82 | 0.199 | 5.8 |
| Cu-ZSM3-5 | 1.38 | 438.23 | 0.189 | 5.7 |
| ImpZSM3-5 | 1.85 | 422.63 | 0.188 | 5.4 |

The $SiO_2$ /$Al_2O_3$ ratio of the catalyst was calculated as 87.2, and the chemical composition of the parent ZSM3-5 catalyst was given in Table 5.6.

Table 5.6. Chemical composition of the parent ZSM3-5 catalyst.

| **Component** | **Mol %** |
|---|---|
| $SiO_2$ | 95.9±4.2 |
| $Al_2O_3$ | 1.1±0.1 |
| $SiO_2$ /$Al_2O_3$ | 87.2 |

IR spectra for each prepared zeolite after pyridine adsorption are shown in Figure 5.9. Again, the same with ZSM2-5 zeolite each spectrum had Brønsted and Lewis acid sites. There is a broad band at 1548 $cm^{-1}$ which is assigned to Brønsted acid sites. The intense band at 1490 $cm^{-1}$ assigned to Brønsted and Lewis acid sites.

However, unlike H-ZSM2-5, H-ZSM3-5 and its cobalt, nickel and zinc loaded forms showed a close acidity. On the other hand ImpZSM3-5 showed the lowest acidity. This shows that some of the acid sites were covered by the impregnation of the Co.

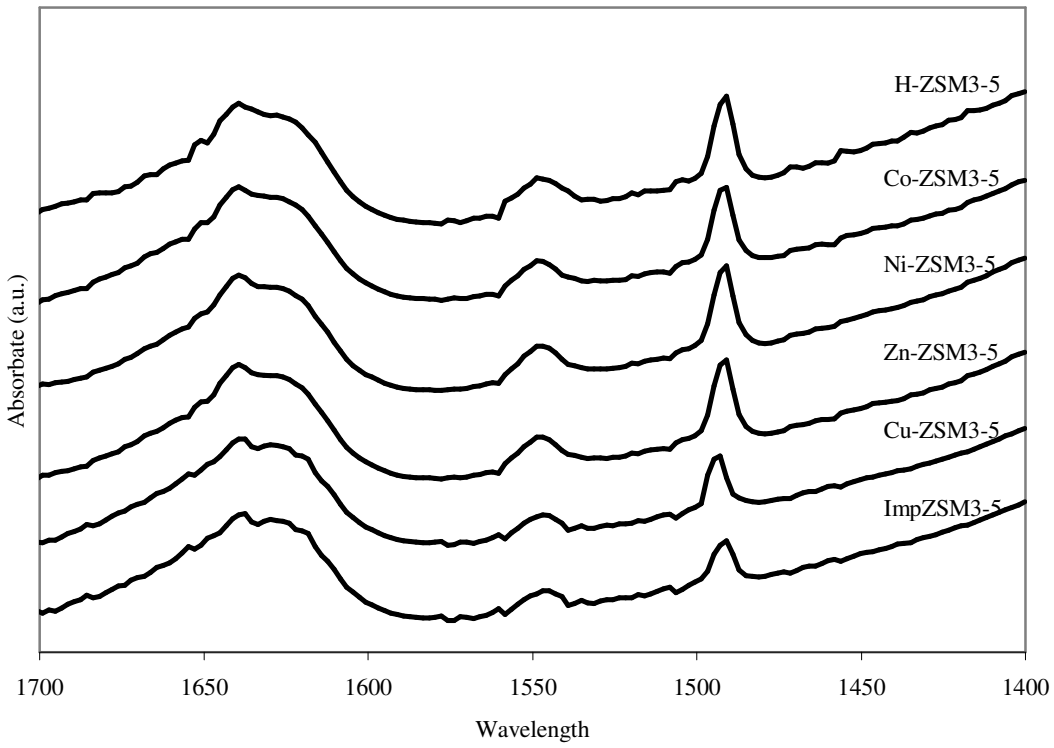


Figure 5.9. IR spectra of pyridine adsorbed metal loaded H-ZSM3-5 catalysts.

## 5.1.2. Ferrierite

The ion exchanged samples were labelled as M-FER where M indicates the metal ion used. The impregnated samples labelled as ImpFER. The XRD patterns of the samples are given in Figure 5.10.

The characteristic peaks of ferrierite zeolite were observed in the XRD patterns for H-FER its modified forms. These patterns are in good agreement with the synthetic ferrierite framework topology. The characteristic peak at 8.9° $2\theta$ confirms the structural stability of the ferrierite zeolite (Khomane et al, 2001). The crystal structure of the zeolite was not affected by metal loadings. This means crystallinity was not destroyed by ion exchange or impregnation of the metal loadings.

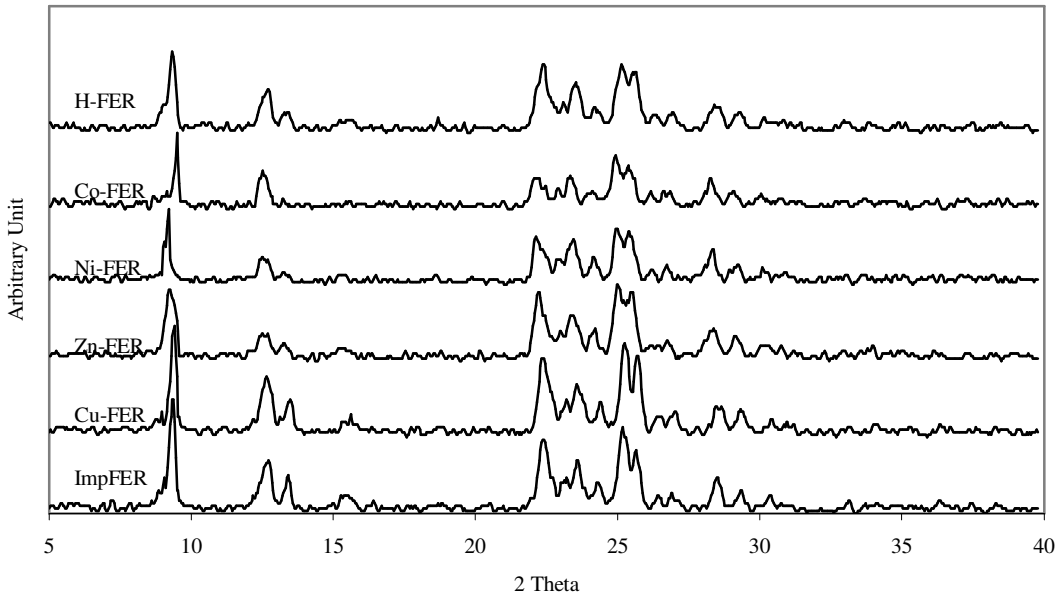


Figure 5.10. XRD patterns of H-FER and its modified samples.

The images of the morphology of some of the catalysts are given in Figure 5.11. The ferrierite had a different morphology than ZSM-5 zeolites. It can be seen that the crystals exhibit rectangular plate type morphology. For ferrierite zeolite crystals a plate like morphology was reported by Smith et al. (1989).

The metal loadings, BET surface areas, Hovarth-Kowazoe pore volumes and median pore diameters of different ferrierite based catalysts were presented in Table 5.7. Metal loadings decreased BET surface areas, H.K. pore volume and H.K. median pore diameter of the catalysts as observed with the ZSM-5 catalysts. Ferrierite catalysts had lower surface area than ZSM-5 catalysts. Their median pore diameter was larger than ZSM2-5 and ZSM3-5, but smaller than ZSM1-5. The lowest results were obtained with the cobalt impregnated catalyst.

Table 5.8 presents the chemical composition of the parent ferrierite catalyst. The $SiO_2$ /$Al_2O_3$ ratio of the catalyst was calculated as 18.9. This measurement is in agreement with the reported values of the manufacturer.

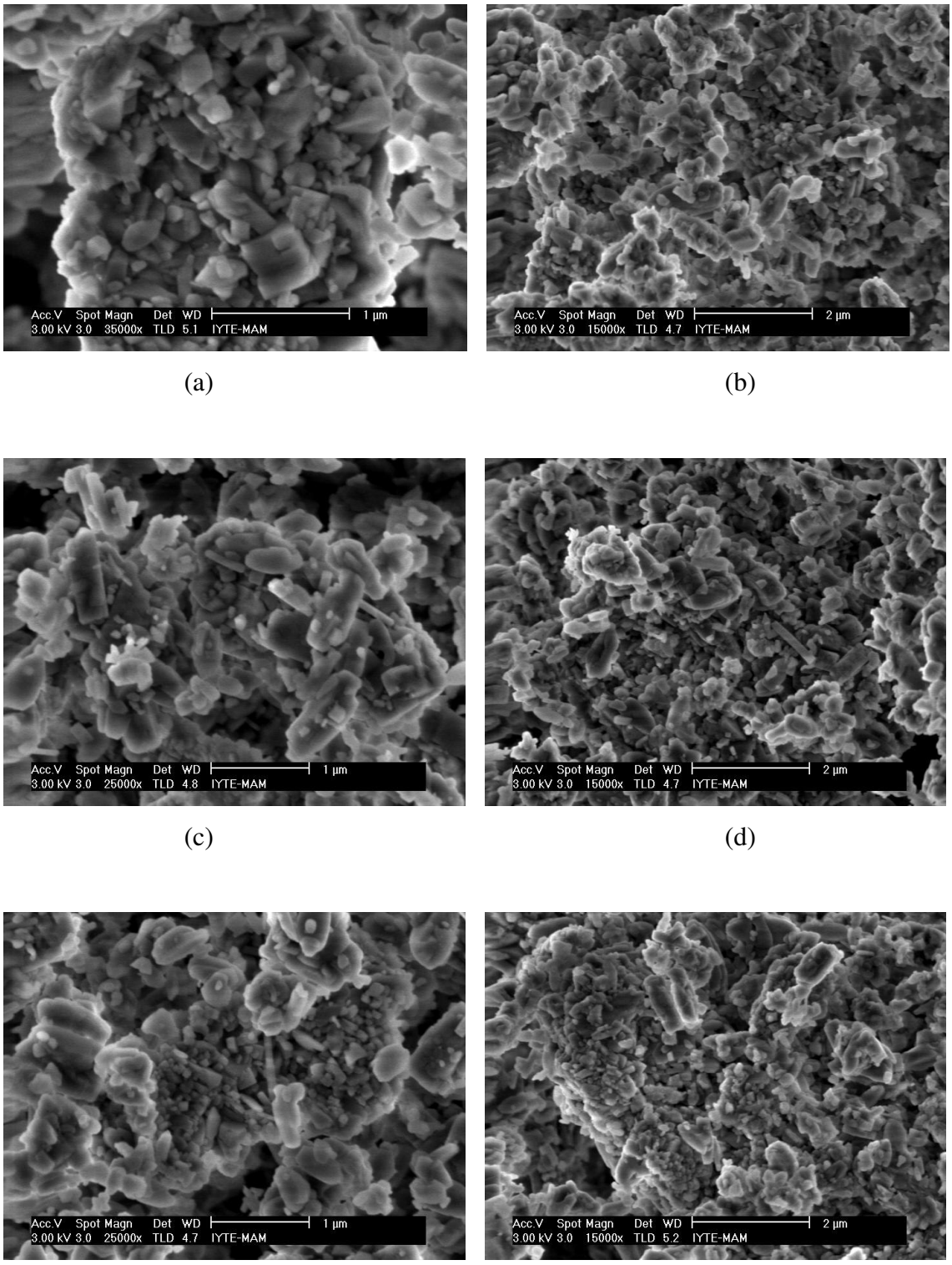


Figure 5.11. SEM images of H-FER and its modified samples. ( a: H-FER, b: Co-FER, c: Ni-FER, d: Zn-FER, e: Cu-FER, f: ImpFER ).

Table 5.7. Textural properties and metal loadings of the ferrierite catalysts.

| Sample | Metal Loading (w%) | BET Surface Area ($m^2/g$) | H.K. Pore volume ($cm^3/g$) | H.K. Median Pore Diameter (Å) |
|---|---|---|---|---|
| H-FER | | 339.25 | 0.172 | 6.2 |
| Co-FER | 1.36 | 332.42 | 0.182 | 6.2 |
| Ni-FER | 1.25 | 335.03 | 0.179 | 6.1 |
| Zn-FER | 1.56 | 330.94 | 0.171 | 6 |
| Cu-FER | 1.57 | 335.1 | 0.173 | 6 |
| ImpFER | 2.02 | 313.06 | 0.158 | 5.7 |

Table 5.8. Chemical composition of the parent ferrierite catalyst.

| **Component** | **Mol %** |
|---|---|
| $SiO_2$ | 85.3±3 |
| $Al_2O_3$ | 4.5±0.3 |
| $SiO_2$ /$Al_2O_3$ | 18.9 |

The acidity of the catalysts determined by pyridine adsorption are given in Figure 5.12. From the spectras, it can be observed that the ferrierite catalysts did not present the band at 1455 $cm^{-1}$ which is related to Lewis acidity. The catalysts present Brønsted and Lewis acid sites. The appearance of the intense band at 1490 $cm^{-1}$ assigned to Brønsted and Lewis acid sites. Also a broad band at 1548 $cm^{-1}$ is present which is assigned to Brønsted acid sites.

Different catalysts showed different acidities. The highest acidity was obtained with H-FER. And the lowest acidity was obtained with ImpFER. The acidities of the ferrierite catalysts decreased with the following order; H-FER > Co-FER > Ni-FER > Zn-FER > Cu-FER > ImpFER.

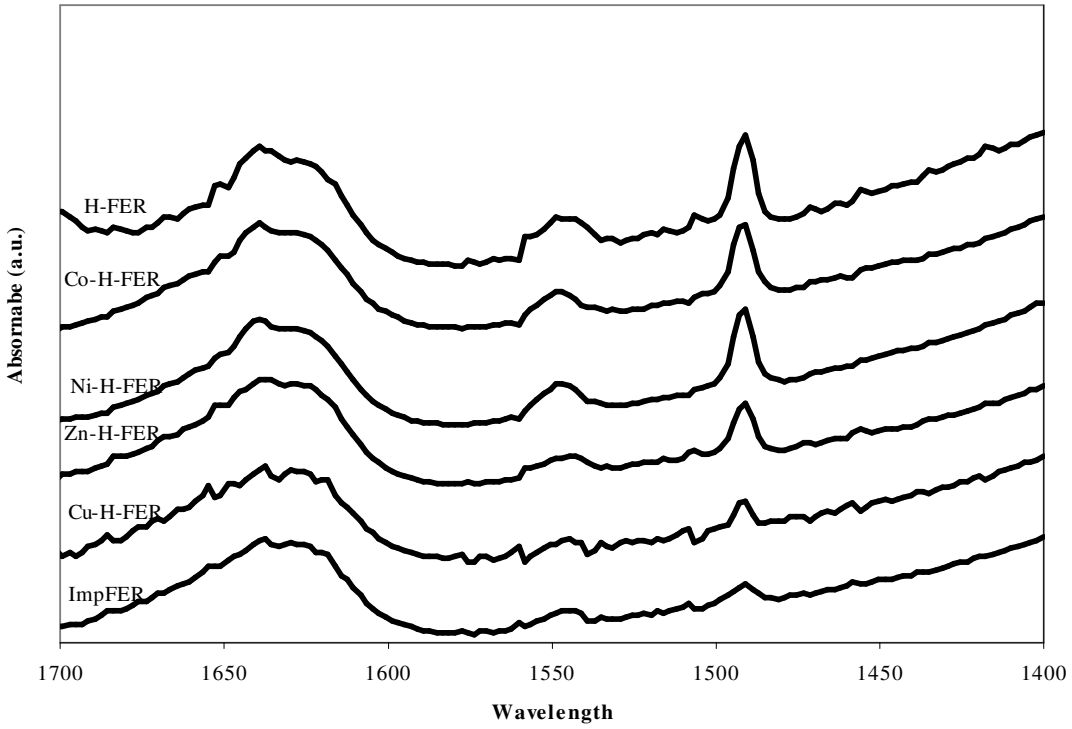


Figure 5.12. IR spectra of pyridine adsorbed metal loaded ferrierite catalysts.

The modifications over the acidity that occurs when a metal is incorporated to an acid support can be due to

(i) blockage of the pore system and superficial sites by large size metallic particles and

(ii) deactivation of acid sites and pore blockage by carbonaceous deposits produced during the precursor compound decomposition in the calcination step that hinder probe molecule from reaching the acid sites. The predominant effect depends on the preparation method and precursor compound used. Thus, the reason for the acidity decrease in the catalysts prepared by incipient wetness impregnation must be the carbonaceous deposits formation when organic precursors are employed (Romero et al, 1997).

## 5.2. Catalyst Testing

Skeletal isomerization of n-butene reactions were performed over different metal loaded catalysts prepared with ion exchange and impregnation method. The reaction temperature and the weight hourly space velocity (WHSV) were taken from a previous study (Demirkan et al, 2002) as 375 °C and 22 $h^{-1}$ respectively.

The double bond isomerization between 1-butene and 2-butene is a very facile reaction and usually reaches equilibrium condition between 1-butene and 2-butenes. So, trans-2 and cis-2 butenes were counted as reactants for the conversion calculation of 1-butene not as products. The conversion of 1-butene is defined as the mass percent of reactant consumed. In addition, the selectivity to isobutene is defined as the mass percent fraction of isobutene to the consumed reactant and calculations were done as follows:

$$Conversion(mass\%) = \frac{(1-butene)_{in} - (n-butene)_{out}}{(1-butene)_{in}} \times 100$$

$$Yields\ of\ isobutene(mass\%) = \frac{(isobutene)_{out}}{(1-butene)_{in}} \times 100$$

$$Selectivity\ to\ isobutene(mass\%) = \frac{(isobutene)_{out}}{(1-butene)_{in} - (n-butene)_{out}} \times 100$$

The following equation shows the relationship between conversion, yield and selectivity;

$$Yield\ of\ isobutene = Conversion \times Selectivity\ to\ isobutene$$

### 5.2.1. Ion Exchange

#### 5.2.1.1. Different Amount of Metal Loadings to ZSM1-5

The conversion to n-butene, selectivity and yield to isobutene obtained with ZSM1-5 having different cobalt loadings are shown in Table 5.9. The best conversion was obtained by 1.45 w% cobalt loaded catalysts (59.1 %). The conversion of 1-butene

increased and passed through a maximum point and then decreased as the metal loading was increased from 0.23 to 2.89 w% as can be seen from Figure 5.13. The increase in cobalt loading lowered conversion as low as 47.1 %. Lee et al (2002) studied effect of metal cation over clinoptilolite on the skeletal isomerization of 1-butene. Their results also showed that increasing the metal loading with ion exchange lowered both conversion and yield of isobutene.

Table 5.9. Conversion, yield of isobutene and selectivity to isobutene over ZSM1-5 zeolite catalysts with different cobalt loadings. (T = 375 °C, WHSV = 22 $h^{-1}$, TOS = 180 min).

| **Catalyst** | **Conversion (%)** | **Selectivity (%)** | **Yield (%)** |
|---|---|---|---|
| 2.89 w% | 47.1 | 37.6 | 17.8 |
| 1.45 w% | 59.1 | 41.4 | 24.5 |
| 0.63 w% | 28.3 | 8.9 | 2.5 |
| 0.23 w% | 27.4 | 1.8 | 0.48 |

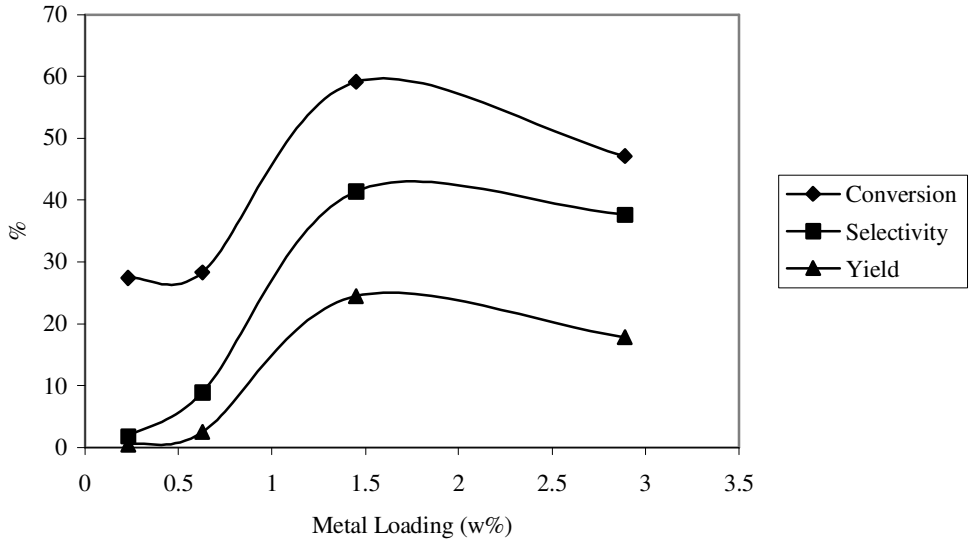


Figure 5.13. Conversion, yield of isobutene and selectivity to isobutene over ZSM1-5 zeolite catalysts with different cobalt loadings.(T = 375 °C, WHSV = 22$h^{-1}$, TOS = 180 min).

The yield of isobutene is greatly affected with different amounts of loadings (Figure 5.14). 1.45 w% Co loaded catalyst showed the highest yield of isobutene at around 24.5 %. Increasing the loading lowered the yield to about 17.8 %. Lowering the metal amount also lowered the yield. Catalysts having 0.63 w% and 0.23 w% Co loadings had 2.5 % and 0.48 % of yield, respectively. This results showed that using metal solution of 0.01 M concentration was good for obtaining better conversions and selectivities. Therefore this concentration was used for all supports that used through the study.

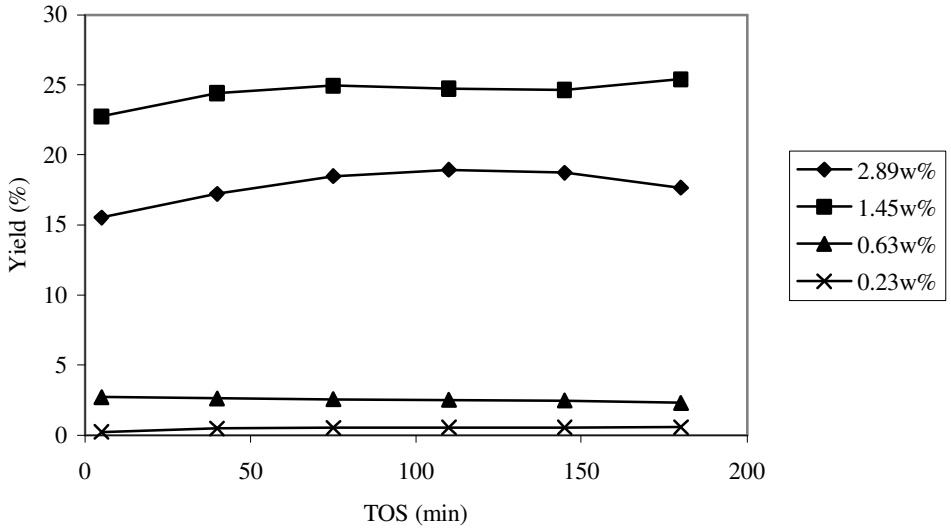


Figure 5.14. Yield of isobutene as a function of TOS over Co loaded ZSM1-5 with different amounts of loadings. (T = 375 °C, WHSV = 22 $h^{-1}$).

## 5.2.1.2. Different Metals Loaded to ZSM1-5

Table 5.10 shows the conversion, selectivity to isobutene and yield of isobutene for H-ZSM1-5 catalysts and its ion exchanged forms. With different metal loadings, different activities were obtained. Figure 5.15 shows the conversion, yield of isobutene and selectivity to isobutene as a function of time on stream (TOS) over H-ZSM1-5. H-ZSM1-5 catalysts showed the best activity for skeletal isomerization of n-butene (59 % conversion, 33.2 % yield). Cobalt and cupper loaded catalysts showed similar conversions with H-ZSM1-5, (59.1 and 60.6 %). But the catalysts showed poor yields for isobutene, Co-ZSM-5 24.5 % and Cu-ZSM-5 25.2 %. This could be caused either by

pore size and acidity. Since Co and Cu forms have smaller pore size, the activity observed can be attributed to the acidity. Brønsted acidity may have decreased more, and lower selectivity to isobutene thus observed.

Table 5.10. Conversion, yield of isobutene and selectivity to isobutene over ZSM1-5 zeolite catalysts. (T = 375 °C, WHSV = 22 $h^{-1}$, TOS = 180 min).

| **Catalyst** | **Conversion (%)** | **Selectivity (%)** | **Yield (%)** |
|---|---|---|---|
| H-ZSM1-5 | 59.0 | 56.4 | 33.2 |
| Co-ZSM1-5 | 59.1 | 41.4 | 24.5 |
| Ni-ZSM1-5 | 53.9 | 43.8 | 23.5 |
| Zn-ZSM1-5 | 49.6 | 43.7 | 21.6 |
| Cu-ZSM1-5 | 60.6 | 41.6 | 25.2 |
| Mn-ZSM1-5 | 33.4 | 28.8 | 9.6 |
| Mg-ZSM1-5 | 37.6 | 32.5 | 12.2 |

Conversion and selectivity to isobutene was lower with Cu, Mn and Mg ion exchanged catalysts. These metals are basic. They most likely have reduced the acidity of the catalysts, so low conversions of n-butene and selectivity to isobutene were obtained.

In Figure 5.16 yields of isobutene as a function of TOS over different metal ion exchanged ZSM1-5 can be seen. Ion exchange with different metals lowered the yield of isobutene. The yield for H-ZSM1-5 was calculated as 33.2 %. However, cobalt, nickel, zinc and cupper loaded catalysts had yields around 20-25 %. The worst activities were obtained by magnesium and manganese loaded ZSM1-5 catalysts. Their conversions were around 35 %, and yields to isobutene were around 10 %.

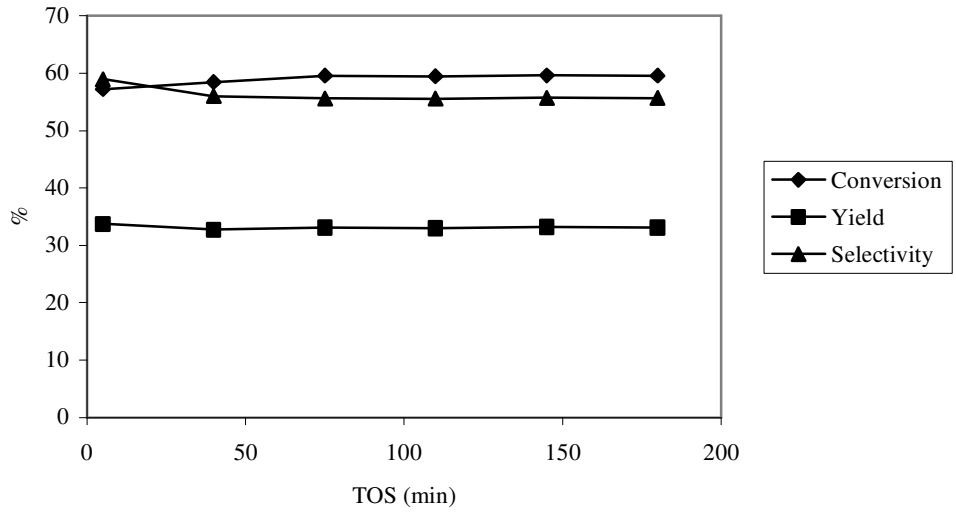


Figure 5.15. Conversion, yield of isobutene and selectivity to isobutene as a function of TOS over H-ZSM1-5 (T = 375 °C, WHSV = 22 $h^{-1}$).

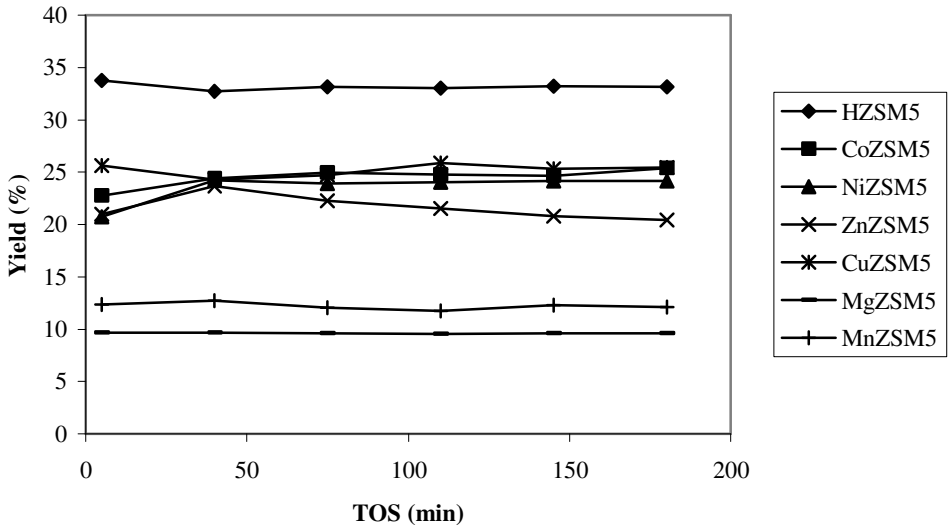


Figure 5.16. Yield of isobutene as a function of TOS over different metal ion exchanged ZSM-5 (T = 375 °C, WHSV = 22 $h^{-1}$).

The metal loadings to H-ZSM-5 did not enhance, but decreased the performance of the catalyst.

The decrease of BET surface area by metal loadings may reduce the space in the interior of zeolite crystals and the oligomers formation inside the pores. The loss of catalytic activity of the modified zeolites may be due to the decreased diffusion rates of *n*-butene molecules through the narrowed pore openings rather than to the loss of acid centers in the zeolite framework. Mériaudeau et al. (1997) have reported that the major factor governing isobutene selectivity is the space available around the active sites.

The products distribution of skeletal isomerization of *n*-butenes to isobutene over ZSM1-5 catalyst with different metal loadings were summarized in Table 5.11. From the table the affect of metal loading can be also seen. The main products of the butene reaction over MFI zeolites are isobutene, pentenes and propene. Metal loaded catalysts had a lower tendency to form alkanes; therefore a subsequent enhancement of isobutene/isobutane ratios is observed. Hydrogen transfer reactions are joined to the aromates and coke formation which is directly related to the distribution of strong acid

Table 5.11. Product distribution of skeletal isomerization of *n*-butenes to isobutene at time on stream 3 h over ZSM1-5 catalyst with different metal loadings.

| | **H** | **Co** | **Ni** | **Zn** | **Cu** | **Mg** | **Mn** |
|---|---|---|---|---|---|---|---|
| **Methane** | - | - | - | - | - | - | - |
| **Ethene** | - | - | - | - | - | - | - |
| **Ethylene** | 0.48 | 0.42 | 1.67 | 0.31 | 0.62 | - | - |
| **Propane** | - | - | - | - | - | - | - |
| **Propylene** | 9.02 | 10.25 | 7.76 | 5.60 | 10.94 | 0.06 | 0.15 |
| **Isobutane** | 0.78 | 0.57 | 0.34 | 0.36 | 0.58 | 0.01 | 0.10 |
| **n-Butane** | 0.71 | 0.58 | 0.34 | 0.29 | 0.63 | 0.07 | 0.07 |
| **Trans-2-Butene** | 21.49 | 23.71 | 26.83 | 29.09 | 22.39 | 39.54 | 37.19 |
| **1-Butene** | 12.05 | 14.70 | 15.79 | 17.26 | 14.12 | 22.67 | 21.77 |
| **Isobutene** | 33.20 | 24.50 | 23.50 | 21.60 | 25.20 | 9.60 | 12.20 |
| **Cis-2-Butene** | 15.01 | 17.15 | 19.22 | 21.00 | 16.04 | 28.19 | 27.75 |
| **1-pentene** | 7.30 | 8.14 | 4.50 | 4.38 | 8.07 | 0.07 | 0.19 |

sites present on the catalyst. This fact was observed in the *n*-butene skeletal isomerization over ZSM-5 zeolites where such reactions are dominant (Canizares et al, 2000).

### 5.2.1.3. Different Metals Loaded to ZSM2-5

Different metals were loaded to ZSM2-5 zeolite, in order to observe metal ion effect on the catalyst. Conversion, yield of isobutene and selectivity to isobutene for parent and ion exchanged ZSM2-5 catalyst were shown in Table 5.12.

H-ZSM2-5 and its modified forms showed quite high conversions. But rather low yields and selectivities were obtained. H-ZSM2-5 showed the highest conversion with 82.7 % (Figure 5.17). At steady state Co-ZSM2-5 showed similar conversion as the parent zeolite with 82.7 %. But if selectivities were considered H-ZSM2-5 is superior, 21.5 %, with respect to 17.9 %. Ni-ZSM2-5 and Zn-ZSM2-5 showed similar conversions around 79 %. The lowest conversion is obtained by Cu-ZSM2-5 with 76.5 %.

Table 5.12. Conversion, yield of isobutene and selectivity to isobutene over ZSM2-5 zeolite catalysts. (T = 375 °C, WHSV = 22 $h^{-1}$, TOS = 180 min).

| **Catalyst** | **Conversion (%)** | **Selectivity (%)** | **Yield (%)** |
|---|---|---|---|
| H-ZSM2-5 | 82.7 | 26.0 | 21.5 |
| Co-ZSM2-5 | 82.7 | 21.7 | 17.9 |
| Ni-ZSM2-5 | 80.5 | 24.8 | 20.0 |
| Zn-ZSM2-5 | 78.5 | 23.3 | 18.9 |
| Cu-ZSM2-5 | 76.5 | 29.3 | 21.0 |

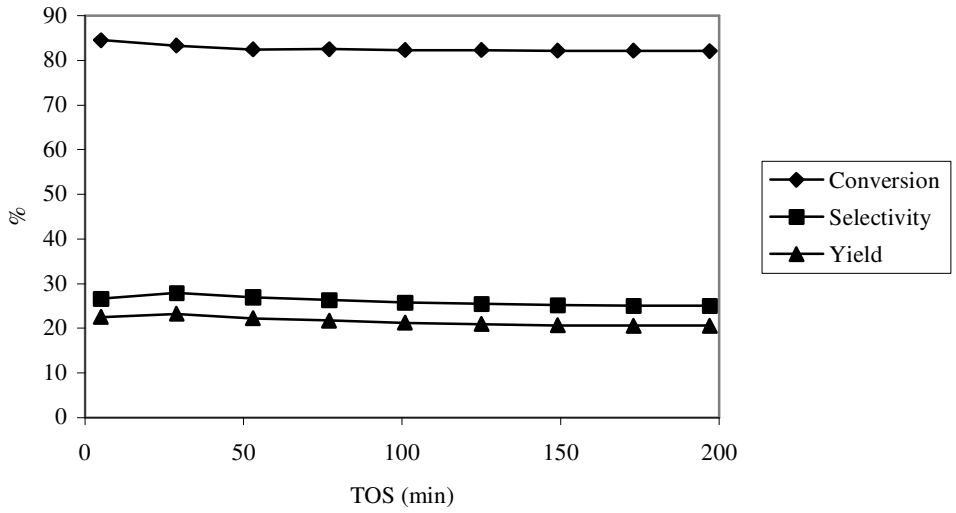


Figure 5.17. Conversion, yield of isobutene and selectivity to isobutene as a function of TOS over H-ZSM2-5 (T = 375 °C, WHSV = 22 $h^{-1}$).

Yield of isobutene over different metal loaded ZSM2-5 catalysts are shown in Figure 5.18. The yield of isobutene was also affected by the metal ion exchang. H-ZSM2-5 showed 21.6 % yield of isobutene. However, in case of metal loadings a decrease was observed. The yields of the metal loaded catalysts were between 17.9 % and 21 %.

According to the findings based on four metal ion studied in this zeolite, it can be said that ion exchange did not improve the performance of the parent zeolite. But some of them showed similar patterns.

Considering the acidity tests made (Figure 5.9), the catalysts having similar acidic properties showed similar catalytic properties. The activity and selectivity of the catalysts decreased with decreasing acidity.

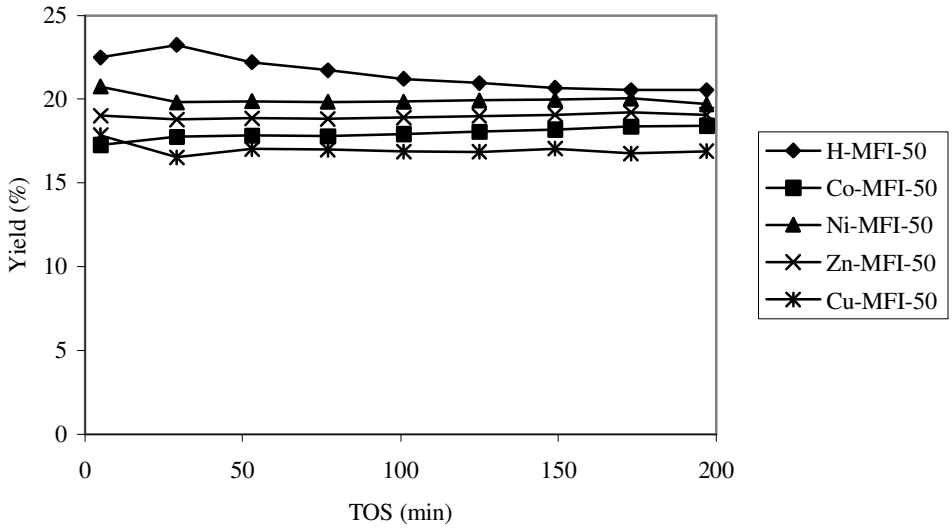


Figure 5.18. Yield of isobutene as a function of TOS over different metal ion exchanged ZSM2-5 (T = 375 °C, WHSV = 22 $h^{-1}$).

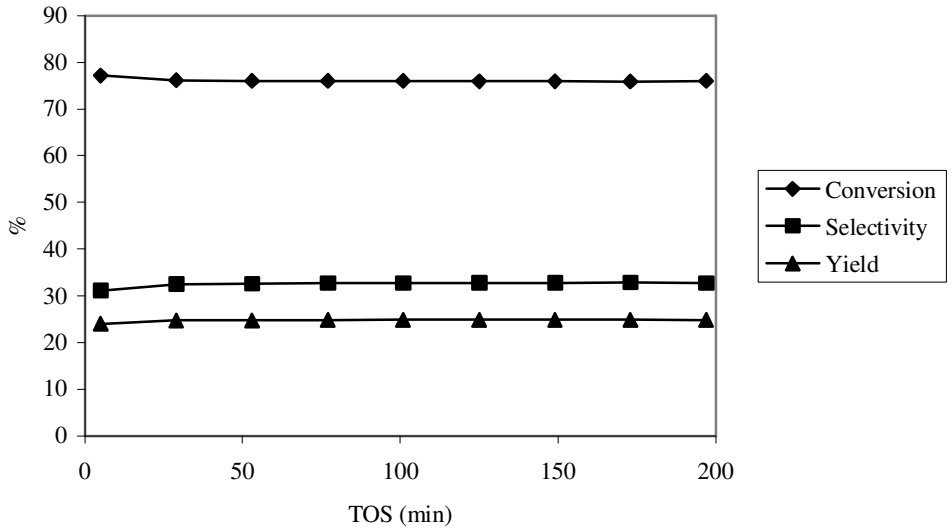


Figure 5.19. Conversion, yield of isobutene and selectivity to isobutene as a function of TOS over H-ZSM3-5 (T = 375 °C, WHSV = 22 $h^{-1}$).

In Table 5.13 product distribution of skeletal isomerization of *n*-butenes to isobutene over ZSM2-5 catalyst with different metal loadings are given. ZSM2-5 catalysts showed higher conversions, but lower yields of isobutene when compared with ZSM1-5 catalysts. The low yield of ZSM2-5 was attributed mainly to the formation of C3 and butane by-products. But, C5+ by-products were not observed. This showed that the reaction mechanism for ZSM2-5 was different from that of ZSM1-5.

Table 5.13. Product distribution of skeletal isomerization of *n*-butenes to isobutene at time on stream 3 h over ZSM2-5 catalyst with different metal loadings.

| | **H** | **Co** | **Ni** | **Zn** | **Cu** |
|---|---|---|---|---|---|
| **Methane** | 0.07 | 0.76 | 0.25 | 0.55 | 0.15 |
| **Ethene** | 0.10 | 0.56 | 0.16 | 0.21 | 0.08 |
| **Ethylene** | 3.36 | 8.90 | 7.80 | 5.08 | 5.69 |
| **Propane** | 3.07 | 5.74 | 4.25 | 2.51 | 2.27 |
| **Propylene** | 18.58 | 25.54 | 27.61 | 15.79 | 28.14 |
| **Isobutane** | 7.63 | 11.35 | 8.59 | 8.33 | 6.17 |
| **n-Butane** | 3.77 | 5.81 | 5.35 | 5.02 | 3.41 |
| **Trans-2-Butene** | 16.25 | 10.14 | 11.38 | 15.05 | 13.32 |
| **1-Butene** | 11.61 | 5.88 | 6.66 | 13.58 | 7.87 |
| **Isobutene** | 21.50 | 17.96 | 19.88 | 18.90 | 21.13 |
| **Cis-2-Butene** | 14.50 | 7.15 | 8.07 | 15.25 | 9.77 |
| **1-pentene** | - | - | - | - | - |

## 5.2.1.4. Different Metals Loaded to ZSM3-5

The results for the effect of different types of metal loading to ZSM3-5 zeolite on conversion, yield of isobutene and selectivity to isobutene can be seen in Table 5.14.

The comparison showed that the conversion of n-butene was almost unaffected with cobalt, nickel and zinc loadings to the parent catalyst. They all showed alike conversions around 75 %. On the other hand, cupper loading drastically decreased conversion as low as 65.9 %. Cupper loading showed a similar behaviour on ZSM2-5

zeolite. Since, these two zeolites, ZSM2-5 and ZSM3-5, have the similar structural properties this kind of a result was expected.

Table 5.14. Conversion, yield of isobutene and selectivity to isobutene over ZSM3-5 zeolite catalysts. (T = 375 °C, WHSV = 22 $h^{-1}$, TOS = 180 min).

| Catalyst | Conversion (%) | Selectivity (%) | Yield (%) |
|---|---|---|---|
| H-ZSM3-5 | 76.1 | 32.5 | 24.8 |
| Co-ZSM3-5 | 75.1 | 36.7 | 27.6 |
| Ni-ZSM3-5 | 75.6 | 30.7 | 23.2 |
| Zn-ZSM3-5 | 74.2 | 32.9 | 24.4 |
| Cu-ZSM3-5 | 65.9 | 31 | 20.4 |

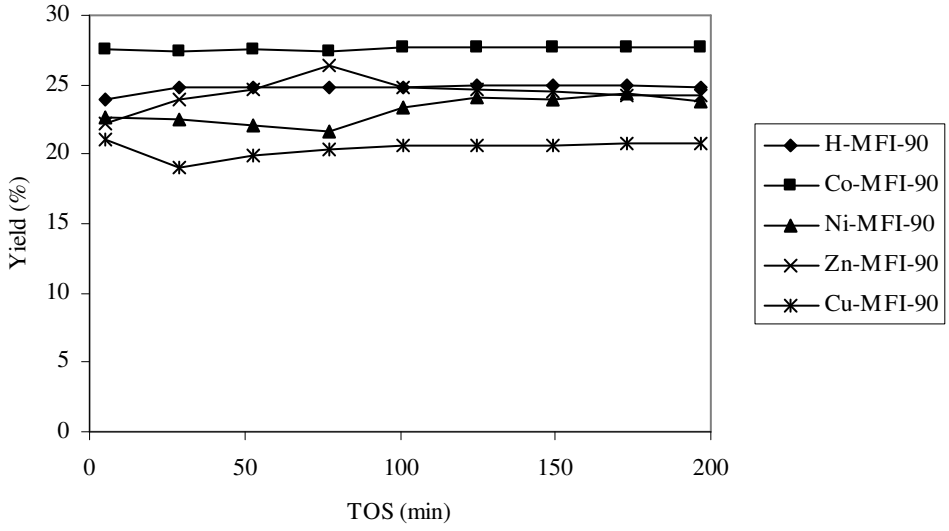


Figure 5.20. Yield of isobutene as a function of TOS over different metal ion exchanged ZSM3-5 (T = 375 °C, WHSV = 22 $h^{-1}$).

In contrast, even though these catalysts showed identical conversions, their selectivities to isobutene were not similar. Co-ZSM3-5 had a higher selectivity (36.7 %) than the rest of the ZSM3-5 catalysts.

In Figure 5.20 yield of isobutene over different metal loaded ZSM3-5 catalysts are shown. Like ZSM2-5, the yield of isobutene was also affected by metal ion exchange. But ZSM3-5 catalysts showed higher yields. H-ZSM3-5 showed 24.8 % yield of isobutene. However, Co-ZSM3-5 had a yield of 27.6 %. In the case of other metals Zn-ZSM3-5 showed same yield with H-ZSM3-5. The worst yield was obtained from cupper loaded catalyst with 20.4 %.

Considering the result obtained from the metal ion exchanged zeolites and the parent zeolite, it can be said that only Co ion exchange improve the performance of the parent zeolite. Similar results were obtained with ZSM2-5 zeolite.

In view of the acidity tests made (Figure 5.13), the catalysts having similar acidic properties showed similar catalytic properties. The activity and selectivity of the catalysts decreased with decreasing acidity. This showed that there is a relation between the acidity and product distribution obtained.

The product distributions of skeletal isomerization of *n*-butenes to isobutene over ZSM3-5 catalyst with different metal loadings were given in Table 5.15. ZSM3-5

Table 5.15. Product distribution of skeletal isomerization of *n*-butenes to isobutene at time on stream 3 h over ZSM3-5 catalyst with different metal loadings.

| | **H** | **Co** | **Ni** | **Zn** | **Cu** |
|---|---|---|---|---|---|
| **Methane** | 0.04 | 0.02 | 0.19 | 0.09 | 0.15 |
| **Ethene** | 0.06 | 0.04 | 0.15 | 0.20 | 0.06 |
| **Ethylene** | 4.52 | 3.04 | 3.64 | 2.25 | 2.88 |
| **Propane** | 1.84 | 2.16 | 2.02 | 1.87 | 1.92 |
| **Propylene** | 28.43 | 23.56 | 30.12 | 22.45 | 31.71 |
| **Isobutane** | 5.03 | 7.76 | 6.73 | 6.89 | 4.95 |
| **n-Butane** | 2.86 | 3.59 | 3.35 | 3.56 | 2.63 |
| **Trans-2-Butene** | 13.83 | 14.81 | 15.89 | 13.65 | 15.56 |
| **1-Butene** | 8.57 | 7.30 | 5.29 | 9.97 | 8.85 |
| **Isobutene** | 24.75 | 27.58 | 23.20 | 24.40 | 20.40 |
| **Cis-2-Butene** | 10.04 | 10.14 | 9.45 | 14.62 | 10.89 |
| **1-pentene** | - | - | - | - | - |

catalysts showed similar product distribution patterns with ZSM2-5 catalysts. Higher yields of propylene was observed for the parent and modified catalysts. Similar with ZSM2-5, C5+ by-products were not observed.

### 5.2.1.5. Different Metals Loaded to Ferrierite

Figures 5.21 through 5.25 shows the conversion of n-butene, selectivity and yield to isobutene obtained with ferrierites having different metal loadings.

As by Canizares et al (2000) and literature reported, ferrierite zeolite did not exhibit enough selectivity to isobutene at the beginning of the reaction. H-FER and its modified forms used in this study showed the same pattern. At the beginning of the reaction higher conversions and lower seletivities were obtained. But as time on stream increased, the conversion decreased, and the selectivity to isobutene increased. Xu et al (2000) also reported that the high isomerization selectivity was achievable only after partial catalyst deactivation by carbonaceous deposits, i.e. coke which poisons strong acid sites and increases spatial constraints limiting n-butene dimerization.

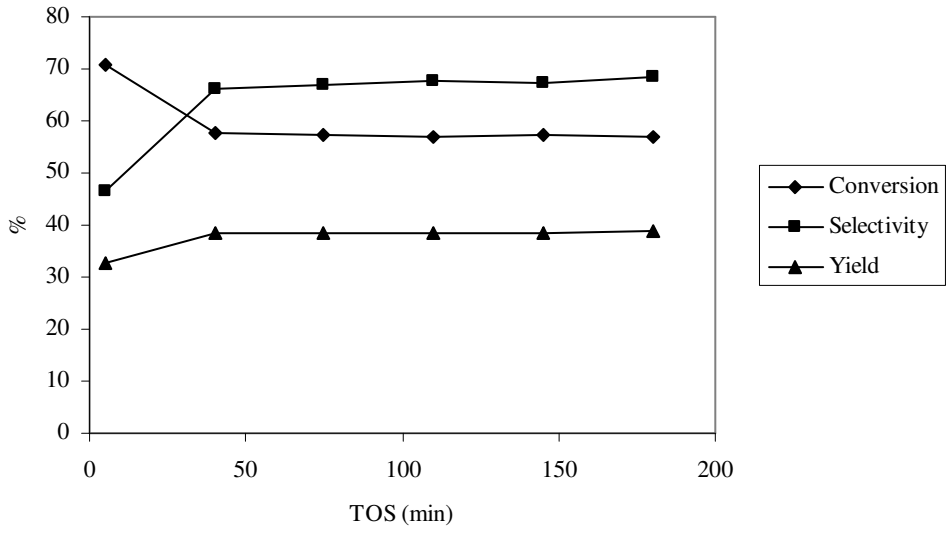


Figure 5.21. Conversion, yield of isobutene and selectivity to isobutene as a function of TOS over H-FER (T = 375 °C, WHSV = 22 $h^{-1}$).

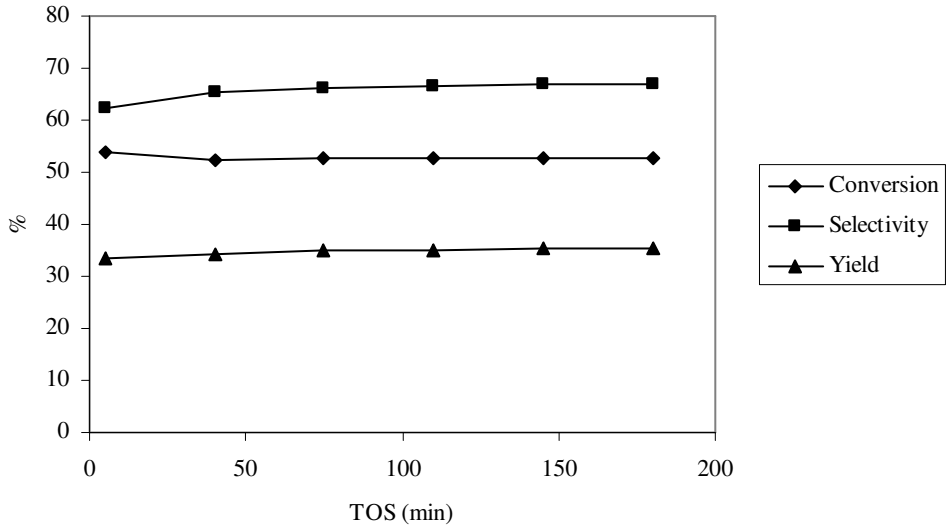


Figure 5.22. Conversion, yield of isobutene and selectivity to isobutene as a function of TOS over Co-FER (T = 375 °C, WHSV = 22 $h^{-1}$).

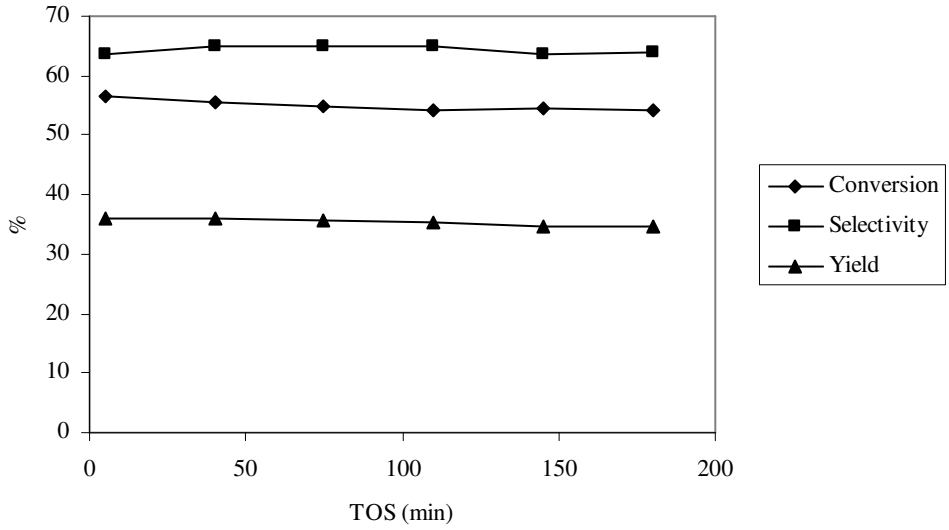


Figure 5.23. Conversion, yield of isobutene and selectivity to isobutene as a function of TOS over Ni-FER (T = 375 °C, WHSV = 22 $h^{-1}$).

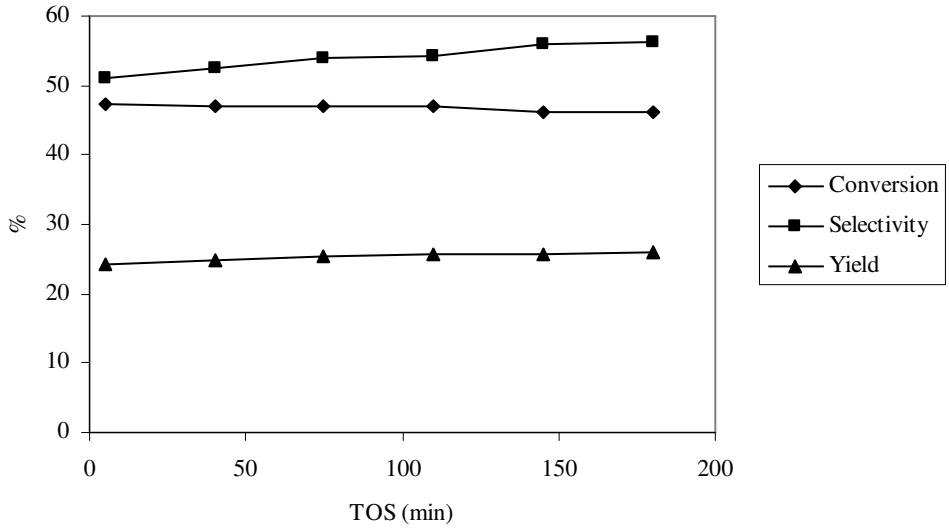


Figure 5.24. Conversion, yield of isobutene and selectivity to isobutene as a function of TOS over Zn-FER (T = 375 °C, WHSV = 22 $h^{-1}$).

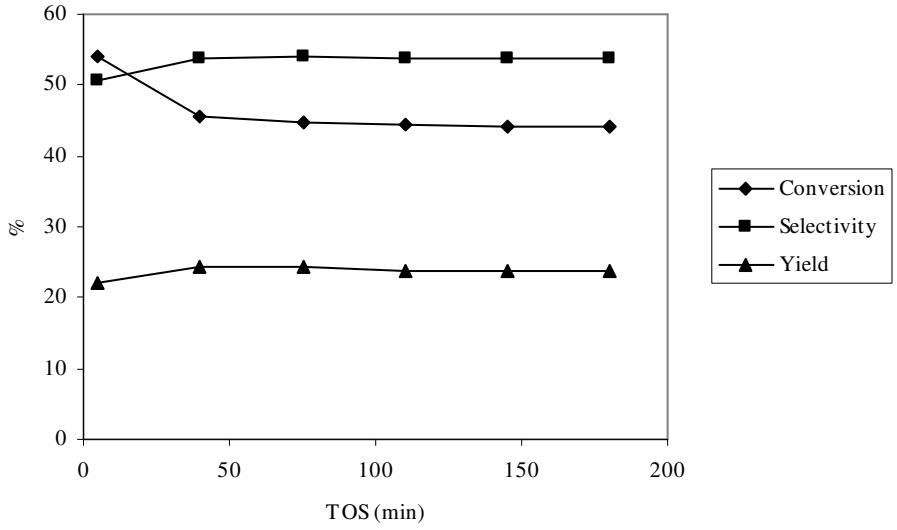


Figure 5.25. Conversion, yield of isobutene and selectivity to isobutene as a function of TOS over Cu-FER (T = 375 °C, WHSV = 22 $h^{-1}$).

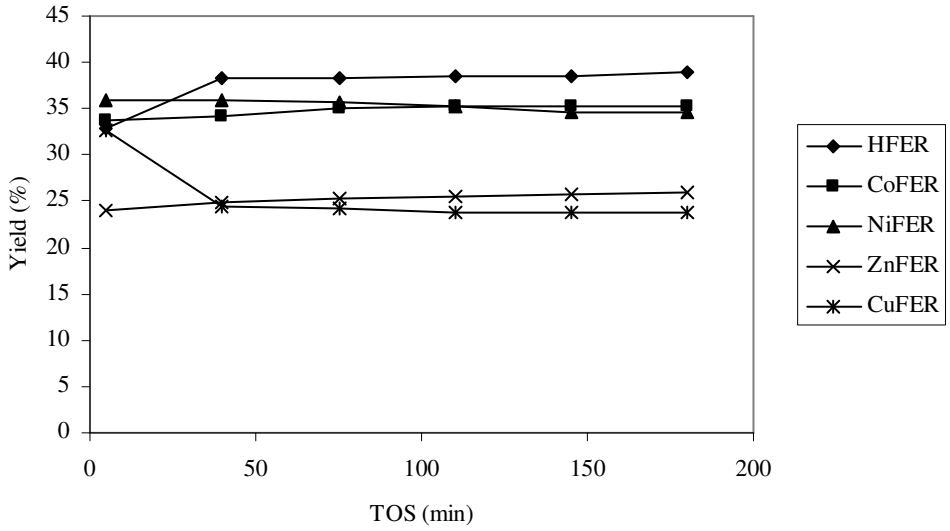


Figure 5.26. Yield of isobutene as a function of TOS over different metal ion exchanged ferrierite (T = 375 °C, WHSV = 22 $h^{-1}$).

As expected, changing the metal ion loaded to the support changed the activity of the catalyst. The highest conversion was obtained by H-FER with 57 % (Figure 5.21). Co-FER and Ni-FER showed similar conversions 52 % and 53 %, respectively (Figures 5.22 and 5.23). Zn-FER and Cu-FER showed the lowest conversions with 47 % and 45 %, respectively (Figure 5.24 and 5.25).

The selectivity to isobutene obtained by H-FER is the highest by 69 %. Ion exchange with other metals lowered the selectivity. Co-FER, Ni-FER, Zn-FER and Cu-FER showed 68 %, 67 %, 58 % and 56 % selectivity to isobutene respectively.

Yield of isobutene over different metal loaded ferrierite catalysts are shown in Figure 5.26. The yield of isobutene also lowered by the ion exchange of different metals. H-FER showed 39 % yield of isobutene. However, Co-FER and Ni-FER had a yield of 37 %. In the case of other metal loadings a much higher decrease was observed (27 %).

In Table 5.16 product distribution of skeletal isomerization of *n*-butenes to isobutene over ferrierite catalyst with different metal loadings are given. Ferrierite

catalysts showed lower conversions when compared with ZSM2-5 and ZSM3-5. However, higher yield of isobutene were obtained.

Table 5.16. Product distribution of skeletal isomerization of *n*-butenes to isobutene at time on stream 3 h over ferrierite catalyst with different metal loadings.

| | **H** | **Co** | **Ni** | **Zn** | **Cu** |
|---|---|---|---|---|---|
| **Methane** | 0.02 | - | 0.01 | 0.01 | 0.01 |
| **Ethene** | - | - | - | - | - |
| **Ethylene** | 0.65 | 0.27 | 0.34 | 0.27 | 0.19 |
| **Propane** | 0.56 | 0.30 | 0.25 | 0.49 | 0.15 |
| **Propylene** | 2.60 | 0.64 | 2.16 | 1.01 | 1.04 |
| **Isobutane** | 0.40 | 0.01 | 0.09 | 0.04 | 0.04 |
| **n-Butane** | 0.38 | 0.21 | 0.50 | 0.29 | 0.21 |
| **Trans-2-Butene** | 24.05 | 27.01 | 26.08 | 30.56 | 29.35 |
| **1-Butene** | 14.05 | 16.01 | 14.03 | 18.24 | 18.08 |
| **Isobutene** | 39.09 | 37.01 | 36.86 | 27.05 | 26.83 |
| **Cis-2-Butene** | 17.45 | 19.06 | 18.22 | 21.25 | 21.56 |
| **1-pentene** | 1.42 | 0.36 | 1.60 | 0.69 | 0.76 |

The catalyst with the most Brønsted acid site was found to be the most active and selective catalyst. Van Donk et al, (2002) studied ferrierite catalysts and their acidities. They reported that as the number of Brønsted acid sites of the catalyst decreased, the conversion of n-butene also decreased.

In Table 5.16 the product distributions of skeletal isomerization of *n*-butenes to isobutene over ferrierite catalyst with different metal loadings were presented. Ferrierite catalysts showed different product distribution behaviour when compared with ZSM-5 catalysts. Unlike, ZSM2-5 and ZSM3-5 catalysts, ferrierite showed low yields to propylene.

## 5.2.2. Impregnation

Cobalt nitrate was impregnated to the synthesized H-ZSM-5 and commercially supplied ZSM2-5, ZSM3-5 and ferrierite zeolites. The conversion, yield of isobutene and selectivity to isobutene are given in Table 5.17.

Table 5.17. Conversion, yield of isobutene and selectivity to isobutene over cobalt impregnated zeolite catalysts. (T = 375 °C, WHSV = 22 $h^{-1}$, TOS=180 min).

| Catalyst | Conversion (%) | Selectivity (%) | Yield (%) |
|---|---|---|---|
| ImpZSM1-5 | 48.1 | 22.9 | 11 |
| ImpZSM2-5 | 66.8 | 20.4 | 13.8 |
| ImpZSM3-5 | 60.7 | 25.6 | 15.5 |
| ImpFER | 45.4 | 30.3 | 13.7 |

Comparing cobalt impregnated and ion exchanged catalysts, in all the zeolites conversion, yield of isobutene and selectivity to isobutene were severely affected. Considering the acidities, this result was not unexpected. The least acidic catalysts were obtained by impregnation.

Sirinivas et al, (2000), as given in the characterization of ZSM-5 zeolite, studied impregnation over ZSM-5 zeolite. In the study, synthesis of 2,3,5-collidine starting with 2-butanone (methyl ethyl ketone), formaldehyde, and ammonia was made. They stated that medium acidity was required for the reaction as for skeletal isomerization of n-butene. They found that impregnation lowered the selectivity. They suggested that, metal cations might partially block the channel and thus control the extent of product selectivity.

Canizares et al (1997), studied n-butane hydroisomerization over Pt/HZSM-5 catalysts. Pt was both ion exchanged and impregnated to the zeolite. They concluded that, the metal incorporation technique has a significant influence on the catalytic properties of Pt/HZSM-5 catalysts. Their results showed that, ion-exchanged catalysts show a higher selectivity to isobutane than impregnated catalysts. They explained this result with the formation of Pt-H adducts, where the isomerization reaction takes place.

# CHAPTER 6

# CONCLUSION

Commercially supplied MFI type and ferrrierite zeolites and synthesized H-ZSM-5 zeolite were modified in order to change their acidities. The prepared catalysts were tested on the skeletal isomerization of n-butene, and the effect of acidity over the reaction was investigated. Zeolites were ion exchanged with Co, Ni, Zn, Cu (Mg and Mn only for synthesized H-ZSM-5) and impregnated with Co.

The particle morphology and crystal structure of the zeolites were not highly effected with ion exchange. On the other hand, impregnation lowered the crystal structure of the catalyst and some deposits were observed on the surface of the catalysts. The surface areas were also decreased with impregnation.

The acidity measurements of the catalysts were made by IR spectroscopy with pyridine adsorption method. The tests showed that acidities of the catalysts were changed with ion exchange and impregnation of metal ions. When the intensities of the peaks for Brønsted acid sites considered, acidity decreased with metal loading to the parent catalyst. The method used for these was able to give an idea for the acidity change of the catalysts with the treatment. But for quantitative measurements further investigations are needed.

The catalytic tests showed that;

For ZSM1-5 samples, the most active amount of cobalt loading found to be 1.45 w%. Increasing or decreasing the reduced the conversion and yield for isobutene. Also, different metals both with ion exchange and impregnation lowered the activity compared to the parent zeolite. For ZSM2-5 and its modified forms showed high conversions compared to ZSM1-5. But low yield were obtained. For ZSM3-5 and its modified samples showed alike conversions, except for Cu loaded catalyst. Similar with ZSM2-5, the yield of isobutene was affected by the metal ion exchanging. However, for Co loaded catalyst yield for isobutene was enhanced. Same with the other metal supports metal ion loading to ferrierite changed the activity of the catalyst. Again, the

highest conversion was obtained by the parent catalyst. Impregnation with Co, severely decreased the activity of the catalysts both compared to H form and ion exchanged form of the catalysts.

# REFERENCES


Ahedi, R.K.; Kotasthane, A.N.; Rao, B.S.; Manna, A.; Kulkarni, B.D.; "Synthesis of Ferrierite-Type Zeolite in the Presence of a Catalytic Amount of Pyrrolidine and Sodium Bis(2-ethylhexyl) Sulfosuccinate", Journal of Colloid and Interface Science, 2001, 236, 47-51.

Asensi, M. A.; Corma, A.; Martínez, A.; Derewinski, M.; Krysciak, J.; Tamhankar, S.S; "Isomorphous substitution in ZSM-22 zeolite. The role of zeolite acidity and crystal size during the skeletal isomerization of n-butene" Applied Catalysis A: General 174 (1998) 163-175

Baeck, S.H.; Lee, W.Y.; "Dealumination of Mg-ZSM-22 and its use in the skeletal isomerization of 1-butene to iso-butene" Applied Catalysis A: General 168 (1998) 171- 177

Bellussi, G.; Giusti, A.; Zanibelli, L. "Dehydroisomerization catalyst and its use in the preparation of isobutene from *n*-butane" U.K. Patent 2,246,524, 1992.

Breck, D.W., Zeolites Molecular Sieves: Structure, Chemistry and Use, Wiley, NY, 1974

Byggningsbacka R.; Kumar, N.; Lindfors, L.E.; "Comparative Study of the Catalytic Properties of ZSM-22 and ZSM-35/Ferrierite Zeolites in the Skeletal Isomerization of 1-Butene" Journal of Catalysis 178, (1998) 611-620

Byggningsbacka R.; Lindfors, L.E.; Kumar N.; "Catalytic Activity of ZSM-22 Zeolites in the Skeletal Isomerization of 1-Butene" Ind. and Eng. Chem Res. 1997, 36, 2990

Cañizares, P.; Lucas, de A.; Dorado, F. & Pérez, D.; "Effect of zeolite pore geometry on isomerization of n-butane" Applied Catalysis A: General 2000, 190:1-2:233-239

D.L. Hoang, H. Berndt, H. Miessner, E. Schereier, J. Völter, H. Lieske, Appl. Catal. A 114 (1994) 295.

Domokos, L.; Lefferts, L.; Seshan, K.; Lercher, J.A.; "The importance of acid site locations for n-butene skeletal isomerization on ferrierite"; Journal of Molecular Catalysis A: Chemical, 2000, 162, 147-157.

Finelli, Z. R.; Querini, C. A.; Comelli, R. A.; “Skeletal Isomerization of linear butenes on tungsten promoted ferrierite” Applied Catalysis A: General, 2003, 247, 143-156.

Gil, A. D´ıaz, L.M. Gand´ıa, M. Montes, Appl. Catal. A 109 (1994) 167.

Houzvicka, J.; Diefenbach, O.; Ponec, V.; “The Role of Bimolecular Mechanism in the Skeletal Isomerisation of n-Butene to Isobutene” Journal of Catalysis, Vol. 164, No. 2, Dec 1996, pp. 288-300

Houzvicka, J.; Hansildaar, S.; Nienhuis, J.G.; Ponec, V.; “ The role of deposits in butene isomerization” Applied Catalysis A: General 176 (1999) 83-89

Houzvicka, J.; Hansildaar, S.; Ponec, V.; “The Shape Selectivity in the Skeletal Isomerisation of n-Butene to Isobutene”, Journal of Catalysis, Vol. 167, No. 1, Apr 1997, pp. 273-278

Houzvicka, J.; Nienhuis, J.G.; Ponec, V.; “The role of the acid strength of the catalysts in the skeletal isomerisation of n-butene” Applied Catalysis A: General 1998, 174:1-2:207-212

J. Cejka, B. Wichterlova and P. Sarv, Appl. Catal. A Gen. 179 (1999) 217.

J. Szabo, J. Perrotey, G. Szabo, J.C. Duchet, D. Cornet, Journal of Molecular Catalysis 67 (1991) 79.

Kumar, N.; “Synthesis, modification and application of high silica zeolite catalysts in the transformation of light hydrocarbons to aromatic hydrocarbons”, Doctoral Thesis, Abo Akademi University 1996.

Lee, H.C.; Woo, H.C.; Chung, S.H.; Kim, H.J.; Lee, K.H.; Lee, J.S.; “Effects of Metal Cation on the Skeletal Isomerization of 1-Butene over Clinoptilolite” Journal of Catalysis, 2002, 211, 216-225.

M. Guisnet, P. Andy, N.S, Gnep, C. Travers and E. Benazzi, Ind. Eng. Chem. Res. 37 (1998) 300.

M. Müller, G. Harvey and R. Prins, Micropor. Mesopor. Mat. 34 (2000) 135.

Meriaudeau, P., Bacaud, R., Hung, L. N., and Vu, A. T., J. Mol. Catal. A 110, L177 (1996).

Nicolaides, C.P.; “A novel family of solid acid catalysts: substantially amorphous or partially crystalline zeolitic materials” Applied Catalysis A: General 1999, 185:2:211- 217

Nieminen, V.; Kumar, N.; Datka, J.; Paivarinta, J.; Hotokka, M.; Laine, E.; Salmi, T.; Murzin, D.Y.; “Active copper species in 1-butene skeletal isomerization:

comparison between copper-modified MCM-41 and beta catalysts" Microporous and Mesoporous Materials, 2003, 60, 159-171.

O'Young, C.; Browne, J. E.; Matteo, J. F.; Sawicki, R. A.; Hazen, J. "Bimetallic catalysts for dehydroisomerization of n-butane to isobutene" U.S. Patent 5,198,597, 1993.

Pal-Borbely, G.; Beyer, H.; Kiyozumi, Y.; Mizukami, F.; "Synthesis and characterization of a ferrierite made by recrystallization of an aluminium-containing hydrated magadiite" Microporous and Mesoporous Materials 1998, 22, 57-68.

Seddon, D. "Reformulated Gasoline, Opportunities for New Technology" Catalysis Today 1992, 15, 1.

Seo, G., Park, S.-H., Kim, J.-H.; The reversible skeletal isomerization between nbutenes and iso-butene over solid acid catalysts" Catalysis Today 44 (1998) 215-222

Sikkenga, D. L.; Nevitt, T. D.; Jerome, N. F. "Process to convert linear alkenes" U.S. Patent 4,433,190, 1984.

Vartuli J.,C.; Kennedy G., J.; Yoon B.,A.; Malek A.; "Zeolite Synthesis using diamined: evidence for in situ directing agent modification" Microporous Materials, Vol. 38 (2000) 247-254

Vartuli, J.C.; Roth, W.J., Beck, J.S., McCullen, S.B.; Kresge, C.T.; In: Molecular Sieves Science & Technology, H.Karge, J. Weitkamp (Eds) 1998 Springer.

Weitkamp, J.; Puppe, L.; (Eds); Catalysis and Zeolites, Fundementals and Applications Springer-Verlag Berlin Heidelberg 1999, preface

Xu, W.-Q.; Yin, Y.-G.; Suib, S. L.; Edwards, J. C.; O'Young, C.-L. "n-Butene Skeletal Isomerization to Isobutylene on Shape Selective Catalysts: Ferrierite/ZSM-35" Journal of Physical Chemistry. 1995, 99, 9443.

Yang, S.-M.; Lin, J.-Y.; Guo, D.-H.; Liaw, S.-G.; "1-Butene isomerization over aluminophosphate molecular sieves and zeolites" Applied Catalysis A: General 1999, 181:1:113-122